

# Fast Variational Block-Sparse Bayesian Learning

Jakob Möderl, Erik Leitinger, Bernard H. Fleury, Franz Pernkopf, and Klaus Witrisal

**Abstract**—We present a variational Bayesian (VB) implementation of block-sparse Bayesian learning (BSBL) which uses the mean-field theory to approximate the posterior probability density function (PDF) of the latent variables in the underlying model with a product of marginal proxy PDFs. The prior distribution of the hyperparameters associated with BSBL is selected to be the generalized inverse Gaussian distribution. This choice unifies commonly used hyperpriors, e.g. the Gamma distribution, inverse Gamma distribution, and Jeffrey’s improper prior. The resulting variational BSBL (VA-BSBL) algorithm updates in an iterative manner the proxy PDFs of the weights and hyperparameters until a convergence criterion is fulfilled.

The proxy PDF of the weights only depends on the proxy PDFs of the hyperparameters through the means of the latter PDFs. Inspired by a previous work on classical sparse Bayesian learning (SBL), we adopt a scheduling of the iterations in which the proxy PDF of a single hyperparameter and the proxy PDF of the weights are cyclically updated *ad infinitum*. The resulting sequence of means of the hyperparameter proxy PDFs computed in this way can be expressed as a nonlinear first-order recurrence relation. Hence, the fixed points of the recurrence relation can be used for single-step check for convergence of this sequence. Including this check procedure in the VA-BSBL, we obtain a fast version of the algorithm, coined fast-BSBL (F-BSBL), which shows a two-order-of-magnitude faster runtime. Additionally, we analyse a necessary condition for the existence of fixed points and show that only certain improper generalized inverse Gaussian hyperpriors induce a sparse estimate of the weights.

For classical SBL, the VB and expectation-maximization (EM)-based Type-II implementations are known to be equivalent. We generalize this equivalence to BSBL. Specifically, we show that the presented VA-BSBL is equivalent to EM-based Type-II-BSBL. As a result, the fast versions of them, i.e. F-BSBL for the former and Type-II-BSBL using coordinate ascent for the latter, are equivalent as well. This result allows for reinterpreting previous works on BSBL within our framework.

## I. INTRODUCTION

Sparse signal models have gained widespread adoption over the last 20 years through the advent of compressed sensing [1]. Generally, the aim of sparse signal reconstruction algorithms is to reconstruct a signal based on a large dictionary matrix as a weighted linear combination of only a few (non-zero) entries of the dictionary. One approach to solve this problem

This research was partly funded by the Austrian Research Promotion Agency (FFG) within the project SEAMAL Front (project number: 880598). Furthermore, the financial support by the Christian Doppler Research Association, the Austrian Federal Ministry for Digital and Economic Affairs and the National Foundation for Research, Technology and Development is gratefully acknowledged.

Jakob Möderl and Klaus Witrisal are with the Institute of Communication Networks and Satellite Communications at Graz University of Technology, Graz Austria.

Erik Leitinger and Franz Pernkopf are with the with the Signal Processing and Speech Communications Laboratory at Graz University of Technology, Graz, Austria.

Bernard H. Fleury is with the Institute of Telecommunications, TU Wien, Vienna, Austria.

Klaus Witrisal and Erik Leitinger are further associated with the Christian Doppler Laboratory for Location-aware Electronic Systems.

is sparse Bayesian learning (SBL). SBL uses the Gaussian scale mixture model [2], which models the prior precision, i.e., inverse variance, of each weight as a hyperparameter.<sup>1</sup> These hyperparameters are estimated from the data, e.g. by maximizing the marginal likelihood [3], the expectation-maximization (EM) algorithm [4], or variational Bayesian (VB) inference [5]. Note, that the former two are instances of Type-II Bayesian inference [6]. A major shortcoming of the SBL framework is the slow convergence of the hyperparameter estimates. However, this problem is alleviated by a “fast” method to maximize the marginal likelihood [7], [8]. Fast updates also have been developed for the EM approach to SBL [9] and the VB approach [5]. In the EM and VB case, fast update rules are obtained via the fixed points of a recurrent relation for the updates of a single hyperparameter.

In classical SBL, all weights in the model are assumed independent. However, some applications result in a block-sparse model in which groups or blocks of weights are jointly zero or nonzero. Naturally, the different approaches to SBL have been extended to such a block structure as well, referred to as block-sparse Bayesian learning (BSBL). For example, [10] extends the Type-II marginal likelihood-based approach to a block structure. Additionally, [10] shows that the hyperparameters can be analytically determined by solving for the roots of a specific polynomial. However, for the application outlined in [10], the degree of this polynomial is considerably large. Therefore, it was not computationally efficient to solve for these roots and an iterative procedure was used instead. In [11], a fast Type-II-BSBL algorithm is presented based on the same polynomial solution as discovered by [10]. Other BSBL approaches include EM-based variants [12], [13], and VB variants [14], [15]. However, these BSBL variants lack a fast update rule and, therefore, suffer from slow convergence.

The EM-based and VB approaches to classical SBL are shown to be equivalent [16]. This equivalence is conceptually relevant as the latter approach can be given a message-passing interpretation, in which messages are proxy probability density functions (PDFs). This interpretation allows for naturally merging classical SBL with other message-passing algorithms such as belief propagation [17], e.g. for joint channel estimation and decoding [18]. Additionally, different hyperpriors, i.e. prior PDFs on the hyperparameters, lead to different estimators. By choosing a parameterized PDF as hyperprior that encompasses many commonly used hyperpriors as special cases of its parameters, we can compare different variants of SBL within the same framework [9], [14]. A fast update rule for the hyperparameters is of critical importance for this analysis. However, extending the fast variational SBL presented in [5] to block-sparse models is not trivial, since [5,

<sup>1</sup>Note that SBL can be derived equivalently by using a hierarchical model on either the prior variances or the prior precisions of the weights.

Theorem 1] merely provides the condition for the existence of one (locally stable) fixed point, whereas multiple fixed points might exist in the block-sparse case.

### Contribution

This work presents three novel theoretical results regarding BSBL.

- We present a variational BSBL (VA-BSBL) algorithm, for which we derive a fast update rule. In particular, we extend and generalize [5, Theorem 1] to block-sparse models, resulting in the proposed fast-BSBL (F-BSBL) algorithm.
- We use a generalized inverse Gaussian (hyper) prior on the BSBL hyperparameters to unify many commonly used hyperprior distributions, e.g. the Gamma distribution, inverse Gamma distribution and Jeffrey's improper prior. Through the recurrent relation at the core of the F-BSBL algorithm, we are able to analyse which parameter settings of the generalized inverse Gaussian hyperprior lead to thresholding behaviour of the estimator, i.e. to a sparse result.
- We show the equivalence between EM-based Type-II-BSBL, e.g. [13], and the variational BSBL (VA-BSBL) algorithm. This result, which is stated in Theorem 3, generalizes the equivalence shown for classical SBL [16] to the block-sparse case. Theorem 3 further implies the equivalence of the F-BSBL algorithm and fast Type-II-BSBL using coordinate ascent, e.g. [11]. Thus, Theorem 3 allows to reinterpret Type-II-BSBL algorithms, e.g. [11] or [13], as VB message-passing algorithms.

In addition to these aforementioned theoretical results, we numerically demonstrate the following advantages of the proposed F-BSBL algorithm.

- The runtime of the F-BSBL algorithm is up to two orders of magnitude shorter than that of similar BSBL algorithms [13] (which is equivalent to a special case of the VA-BSBL algorithm), while simultaneously achieving a better performance in terms of the normalized mean squared error (NMSE) and the probability of correctly recovering the support.
- We apply the F-BSBL algorithm to a direction of arrival (DOA) estimation problem and show the benefits compared to the multi-snapshot SBL-based DOA estimation algorithm in [19].

## II. OVERVIEW OF THE BSBL FRAMEWORK

### A. System Model

We aim to estimate the weights  $\mathbf{x}$  in the linear model

$$\mathbf{y} = \Phi \mathbf{x} + \mathbf{v} \quad (1)$$

where  $\mathbf{y}$  is the observed signal vector of length  $N$ ,  $\Phi$  is an  $N \times M$  dictionary matrix and  $\mathbf{v}$  is additive white Gaussian noise (AWGN) with precision  $\lambda \in \mathbb{R}_{++}$ . Thus, the likelihood function is given by the PDF  $p(\mathbf{y}|\mathbf{x}, \lambda) = \mathcal{N}(\mathbf{y}; \Phi \mathbf{x}, \lambda^{-1} \mathbf{I})$ .<sup>2</sup>

<sup>2</sup>We denote the multivariate Gaussian PDF of the variable  $\mathbf{x}$  with mean  $\boldsymbol{\mu}$  and covariance  $\boldsymbol{\Sigma}$  as  $\mathcal{N}(\mathbf{x}; \boldsymbol{\mu}, \boldsymbol{\Sigma}) = |\frac{\pi}{\rho} \boldsymbol{\Sigma}|^{-\rho} \exp\{-\rho(\mathbf{x} - \boldsymbol{\mu})^H \boldsymbol{\Sigma}^{-1}(\mathbf{x} - \boldsymbol{\mu})\}$ , where  $|\cdot|$  denotes the matrix determinant.

To allow for both a real-valued and complex-valued signal model, we use a likelihood function that is parameterized by  $\rho = \frac{1}{2}$  for the real valued case and  $\rho = 1$  for the complex valued case.

We assume that  $\mathbf{x}$  is block-sparse, meaning that the length- $M$  vector  $\mathbf{x}$  is partitioned into  $K$  blocks  $\mathbf{x}_i$  of weights of known size  $d_i$  each,  $i = 1, \dots, K$ , such that all elements within a block are simultaneously zero or nonzero (with probability one), e.g.

$$\mathbf{x} = \underbrace{[x_1 \ x_2 \ \dots \ x_{d_1}]}_{\mathbf{x}_1^T = \mathbf{0}^T} \underbrace{\dots}_{\mathbf{x}_2^T \neq \mathbf{0}^T} \dots \underbrace{[x_{M-d_K+1} \ \dots \ x_M]}_{\mathbf{x}_K^T = \mathbf{0}^T}^T. \quad (2)$$

The block-sparse model arises in many applications, e.g. the estimation of block-sparse channels in multiple-input–multiple-output communication systems [20], [21], or DOA estimation using the multiple measurement vector (MMV) model [19]. We provide an example of how to apply the system model in (3) to MMV-DOA estimation in Section VIII. In the MMV case, the signal is signal modeled as

$$\mathbf{Y} = \Psi \mathbf{X} + \mathbf{V} \quad (3)$$

where  $\mathbf{Y} = [\mathbf{y}_1 \ \mathbf{y}_2 \ \dots \ \mathbf{y}_J]$  is a matrix of  $J$  measurement vectors  $\mathbf{y}_j$ ,  $\Psi$  is some dictionary matrix with corresponding weights  $\mathbf{X}$ , and  $\mathbf{V}$  is a matrix of additive noise. A common assumption is that the sparsity profile is the same for each column in  $\mathbf{X}$ , i.e. that all elements in each row of  $\mathbf{X}$  are either jointly zero or nonzero. Finding the row-sparse matrix  $\mathbf{X}$  in (3) is equivalent to finding the block-sparse weight vector  $\mathbf{x}$  in (1), where  $\mathbf{y} = \text{vec}(\mathbf{Y}^T)$ ,  $\mathbf{x} = \text{vec}(\mathbf{X}^T)$ ,  $\mathbf{v} = \text{vec}(\mathbf{V}^T)$ , and  $\Phi = \Psi \otimes \mathbf{I}_J$  is the Kronecker product of  $\Psi$  with the  $J \times J$  identity matrix  $\mathbf{I}_J$ . Here  $\text{vec}(\mathbf{X})$  denote the operation of stacking all the columns of the  $N \times M$  matrix  $\mathbf{X}$  into an  $NM \times 1$  column vector.

### B. BSBL Probabilistic Model

BSBL solves the sparse signal reconstruction task of (1) through the method of automatic relevance determination [3]. We use a Gaussian scale mixture model [2]. Each block weight  $\mathbf{x}_i$ ,  $i = 1, \dots, K$  is Gaussian distributed with PDF

$$p(\mathbf{x}_i|\gamma_i) = \mathcal{N}(\mathbf{x}_i; \mathbf{0}, (\gamma_i \mathbf{D}_i)^{-1}), \quad (4)$$

i.e. with zero-mean and with precision matrix  $\gamma_i \mathbf{D}_i$ , where  $\mathbf{D}_i$  with  $\text{tr}\{\mathbf{D}_i\} = 1$  is a known matrix characterizing the intra-block correlation and  $\gamma_i \in \mathbb{R}_{++}$  is a scaling hyperparameter [4], [7], [8]. Given the hyperparameter vector  $\boldsymbol{\gamma}$  the different blocks of weights  $\mathbf{x}_i$  are conditionally independent, i.e.  $p(\mathbf{x}|\boldsymbol{\gamma}) = \prod_{i=1}^K p(\mathbf{x}_i|\gamma_i)$  with  $\boldsymbol{\gamma} = [\gamma_1 \ \gamma_2 \ \dots \ \gamma_K]^T$ . By estimating  $\boldsymbol{\gamma}$  from the data, the relevance of each block is automatically determined. The hyperparameter estimate of many blocks diverges to infinity. These blocks are effectively removed from the model as the corresponding weights approach zero.

To perform (approximate) Bayesian inference, we assume the hyperparameters to be independent, identically distributed according to a (hyperprior) distribution with PDF  $p(\boldsymbol{\gamma})$ , i.e.  $p(\boldsymbol{\gamma}) = \prod_{i=1}^K p(\gamma_i)$ . With the above assumptions the

(marginal) prior of the weights has PDF  $p(\mathbf{x}) = \prod_{i=1}^K p(\mathbf{x}_i)$ , where

$$p(\mathbf{x}_i) = \int p(\mathbf{x}_i|\gamma_i)p(\gamma_i) d\gamma_i. \quad (5)$$

Hence, by specifying different hyperprior PDFs  $p(\gamma)$ , we obtain different marginal priors  $p(\mathbf{x}_i)$ ,  $i = 1, \dots, K$  and, thus, different estimators of the block weights. Commonly used hyper priors include the Gamma and inverse Gamma distributions as well as Jeffrey's improper prior with density  $p(\gamma) \propto \gamma^{-1}$  [5], [9], [14]. The generalized inverse Gaussian distribution includes these distributions as special cases for particular settings of its parameters. Furthermore, the generalized inverse Gaussian distribution is conjugate for the likelihood  $\gamma_i \mapsto p(\mathbf{x}_i|\gamma_i)$ , which allows to solve the VB updates analytically [14]. The PDF of the generalized inverse Gaussian distribution is given by [22]

$$p(\gamma; a, b, c) = \frac{\left(\frac{a}{b}\right)^{\frac{c}{2}} \gamma^{c-1}}{2K_c(\sqrt{ab})} \exp\left\{-\frac{1}{2}(a\gamma + b\gamma^{-1})\right\} \quad (6)$$

with  $c \in \mathbb{R}$  and  $K_\alpha(\cdot)$  denotes the modified Bessel function of the second kind. The density (6) defines a proper (a probability) distribution when, given  $c$ , the parameters  $a$  and  $b$  are restricted such that  $(a, b) \in \Theta_c$ , where

$$\Theta_c = \begin{cases} \{(a, b) : a > 0, b \geq 0\} & \text{if } c > 0 \\ \{(a, b) : a > 0, b > 0\} & \text{if } c = 0 \\ \{(a, b) : a \geq 0, b > 0\} & \text{if } c < 0 \end{cases}. \quad (7)$$

However, we will also consider improper hyperpriors, such as Jeffrey's prior that results with the setting  $a = b = c = 0$ , by allowing  $a$  and  $b$  to range in  $\mathbb{R}_+$  (and  $c$  in  $\mathbb{R}$ ), as long as all proxy densities  $q_{\gamma_i}$  (introduced in Section II-C) are PDFs. Inserting (6) into (5) yields the PDF

$$p(\mathbf{x}_i) \propto \frac{K_{-(c+\rho d_i)}\left(\sqrt{b(a + \mathbf{x}_i^H \mathbf{D}_i \mathbf{x}_i)}\right)}{\left(\sqrt{b(a + \mathbf{x}_i^H \mathbf{D}_i \mathbf{x}_i)}\right)^{c+\rho d_i}} \quad (8)$$

of the generalized hyperbolic distribution [14].

To complete the Bayesian model, we also need a prior distribution for the noise precision  $\lambda$ . We use a Gamma distribution with PDF

$$p(\lambda; \epsilon, \eta) = \frac{\eta^\epsilon}{\Gamma(\epsilon)} \lambda^{\epsilon-1} \exp\{-\eta\lambda\} \quad (9)$$

where  $\epsilon \in \mathbb{R}_{++}$  and  $\eta \in \mathbb{R}_{++}$  are, respectively, the shape and the rate parameters and  $\Gamma(\cdot)$  denotes the Gamma function. The Gamma distribution is conjugate for the precision of a Gaussian distribution.

### C. Variational Bayesian Inference

We apply VB inference [23] [24, Ch. 10] to approximate the posterior PDF

$$p(\mathbf{x}, \boldsymbol{\gamma}, \lambda | \mathbf{y}) \propto p(\mathbf{y} | \mathbf{x}, \lambda) p(\mathbf{x} | \boldsymbol{\gamma}) p(\boldsymbol{\gamma}) p(\lambda) \quad (10)$$

of the parameter vector  $(\mathbf{x}, \boldsymbol{\gamma}, \lambda)$  with a "simpler" proxy PDF  $q(\mathbf{x}, \boldsymbol{\gamma}, \lambda)$ . Specifically, we apply the structured mean-field theory and postulate that  $q(\mathbf{x}, \boldsymbol{\gamma}, \lambda)$  factorizes according to

$$q(\mathbf{x}, \boldsymbol{\gamma}, \lambda) = q_{\mathbf{x}}(\mathbf{x}) q_{\lambda}(\lambda) \prod_{i=1}^K q_{\gamma_i}(\gamma_i). \quad (11)$$

The factors in (11) maximize an evidence lower bound (ELBO) or equivalently minimize the Kullback-Leibler (KL)-divergence between the true posterior  $p(\mathbf{x}, \boldsymbol{\gamma}, \lambda | \mathbf{y})$  and the proxy PDF  $q(\mathbf{x}, \boldsymbol{\gamma}, \lambda)$  [23] [24, Ch. 10]. They are the solutions to the set of implicit equations<sup>3</sup>

$$q_\iota \propto \exp\left\{\left\langle \ln p(\mathbf{x}, \boldsymbol{\gamma}, \lambda | \mathbf{y}) \right\rangle_{q_\iota}\right\}, \quad q_\iota \in \mathcal{Q} \quad (12)$$

where  $\mathcal{Q} = \{q_{\mathbf{x}}, q_{\lambda}, q_{\gamma_1}, q_{\gamma_2}, \dots, q_{\gamma_K}\}$ ,  $q_{\bar{\iota}} = \prod_{q_{\iota'} \in \mathcal{Q} \setminus \{q_{\bar{\iota}}\}} q_{\iota'}$  denotes the product of all factors in  $\mathcal{Q}$  but  $q_{\bar{\iota}}$ , and  $\langle \cdot \rangle_{\bar{q}}$  denotes the expectation of the function given as argument in the brackets with respect to the probability distribution with PDF  $\bar{q}$ .

*Implicit equation for  $q_{\lambda}$ :* By considering  $q_\iota = q_{\lambda}$  in (12) we obtain

$$q_{\lambda}(\lambda) \propto \lambda^{\hat{\epsilon}-1} \exp\{-\hat{\eta}\lambda\}, \quad (13)$$

i.e. a Gamma PDF with shape  $\hat{\epsilon} = \rho N + \epsilon$  and rate  $\hat{\eta} = \rho(\|\mathbf{y} - \boldsymbol{\Phi}\hat{\mathbf{x}}\|^2 + \text{tr}(\boldsymbol{\Phi}^H \boldsymbol{\Phi} \hat{\boldsymbol{\Sigma}})) + \eta$ . The expectation  $\hat{\lambda} = \langle \lambda \rangle_{q_{\lambda}}$  reads

$$\hat{\lambda} = \frac{\rho N + \epsilon}{\rho(\|\mathbf{y} - \boldsymbol{\Phi}\hat{\mathbf{x}}\|^2 + \text{tr}(\boldsymbol{\Phi}^H \boldsymbol{\Phi} \hat{\boldsymbol{\Sigma}})) + \eta}. \quad (14)$$

*Implicit equation for  $q_{\mathbf{x}}$ :* Similarly, by considering  $q_\iota = q_{\mathbf{x}}$  in (12) we get  $q_{\mathbf{x}}(\mathbf{x}) = \mathcal{N}(\mathbf{x}; \hat{\mathbf{x}}, \hat{\boldsymbol{\Sigma}})$  with  $\hat{\mathbf{x}}$  and  $\hat{\boldsymbol{\Sigma}}$  given by

$$\hat{\mathbf{x}} = \hat{\lambda} \hat{\boldsymbol{\Sigma}} \boldsymbol{\Phi}^H \mathbf{y} \quad \text{and} \quad \hat{\boldsymbol{\Sigma}} = (\hat{\lambda} \boldsymbol{\Phi}^H \boldsymbol{\Phi} + \mathbf{D}_{\hat{\gamma}})^{-1}, \quad (15)$$

respectively, where  $\mathbf{D}_{\hat{\gamma}}$  is a block-diagonal matrix with the principal diagonal blocks  $\hat{\gamma}_i \mathbf{D}_i$  where  $\hat{\gamma}_i = \langle \gamma_i \rangle_{q_{\gamma_i}}$ ,  $i = 1, \dots, K$ . [14].

*Implicit equation for  $q_{\gamma_i}$ :* Finally, by considering  $q_\iota = q_{\gamma_i}$ ,  $i = 1, \dots, K$  in (12) we show that

$$q_{\gamma_i}(\gamma_i) \propto \gamma_i^{c_i-1} \exp\left\{-\frac{1}{2}(\hat{a}_i \gamma_i + b \gamma_i^{-1})\right\}, \quad (16)$$

i.e.  $q_{\gamma_i}(\gamma_i)$  equals the PDF of a generalized inverse Gaussian distribution with parameters [14]

$$\hat{a}_i = 2\rho \langle \mathbf{x}_i^H \mathbf{D}_i \mathbf{x}_i \rangle_{q_{\mathbf{x}}} + a, \quad b, \quad c_i = c + \rho d_i. \quad (17)$$

For the update of the other factors in  $\mathcal{Q}$ , only the expectations  $\hat{\gamma}_i = \langle \gamma_i \rangle_{q_{\gamma_i}}$ ,  $i = 1, \dots, K$  are required. From (17) we find that  $\hat{a}_i > 0$ . It follows from (7), that each proxy PDF  $q_{\gamma_i}$  is a proper generalized inverse Gaussian distributions if either  $b > 0$  or  $c > -\rho d_i$ . In this case, the expectation  $\hat{\gamma}_i$  can be computed to be [14], [22]

$$\hat{\gamma}_i = \langle \gamma_i \rangle_{q_{\gamma_i}} = \sqrt{\frac{b}{\hat{a}_i}} \frac{K_{c_i+1}(\sqrt{\hat{a}_i b})}{K_{c_i}(\sqrt{\hat{a}_i b})}. \quad (18)$$

Simplified expressions of the right-hand side in (18) for particular selections of the prior parameters  $a$ ,  $b$  and  $c$  that yield, respectively, the Gamma distribution, the inverse Gamma distribution, and Jeffrey's improper distribution are listed in the third column of Table I.

An iterative algorithm for computing the optimal solutions in (12), or equivalently in (14), (15), and (18), with  $i = 1, \dots, K$  for the latter, is obtained as follows: Estimates of the factors in  $\mathcal{Q}$  are first initialized and then by cycling

<sup>3</sup>In the following we use  $q_\iota$  as a shorthand for  $q_\iota(\iota)$  with  $\iota \in \{\mathbf{x}, \lambda, \gamma_1, \gamma_2, \dots, \gamma_K\}$ .

TABLE I  
FAST UPDATE RULES OF  $\hat{\gamma}_i$  FOR DIFFERENT PARAMETRIZATIONS OF  $p(\gamma)$ , EXPANDING ON [14, TABLE 1]\*

Hyperprior Parameters	Hyperprior Shape	Update of $\hat{\gamma}_i$	$f_i(\gamma)$	Fast Update Polynomial $G_i(\gamma)$	Sparse
$b > 0$ or $c > -\rho d_i$	Generalized inverse Gaussian	$\sqrt{\frac{b}{\hat{a}_i}} \frac{K_{c_i+1}(\sqrt{\hat{a}_i b})}{K_{c_i}(\sqrt{\hat{a}_i b})}$	Eq. (19)	-	If both $a=0$ and $c \geq 0$
$a = 0, b > 0, c = -\rho d_i - \frac{1}{2}$	Inverse Gamma <sup>†</sup>	$\sqrt{\frac{b}{2\rho \langle \mathbf{x}_i^H \mathbf{D}_i \mathbf{x}_i \rangle_{q_{\mathbf{x}}}}}$	$\sqrt{\frac{b A_i(\gamma)}{2\rho B_i(\gamma)}}$	$b A_i(\gamma) - 2\rho \gamma^2 B_i(\gamma)$	No
$a > 0, b = 0, c > -\rho d_i$	Gamma if $c > 0$	$\frac{c + \rho d_i}{\rho \langle \mathbf{x}_i^H \mathbf{D}_i \mathbf{x}_i \rangle_{q_{\mathbf{x}}} + \frac{a}{2}}$	$\frac{c + \rho d_i}{\rho \frac{B_i(\gamma)}{A_i(\gamma)} + \frac{a}{2}}$	$(c + \rho d_i) A_i(\gamma) - \gamma (\rho B_i(\gamma) + \frac{a}{2} A_i(\gamma))$	No
$a = b = 0, c > -\rho d_i$	Scaled Jeffrey's $p(\gamma) \propto \gamma^{c-1}$	$\frac{c + \rho d_i}{\rho \langle \mathbf{x}_i^H \mathbf{D}_i \mathbf{x}_i \rangle_{q_{\mathbf{x}}}}$	$\frac{c + \rho d_i}{\rho \frac{B_i(\gamma)}{A_i(\gamma)}}$	$(c + \rho d_i) A_i(\gamma) - \rho \gamma B_i(\gamma)$	If $c \geq 0$
$a = b = c = 0$	Jeffrey's $p(\gamma) \propto \gamma^{-1}$	$\frac{d_i}{\langle \mathbf{x}_i^H \mathbf{D}_i \mathbf{x}_i \rangle_{q_{\mathbf{x}}}}$	$\frac{d_i A_i(\gamma)}{B_i(\gamma)}$	$d_i A_i(\gamma) - \gamma B_i(\gamma)$	Yes

\* Note, that our model is slightly different from the one used in [14]. The hyperparameters  $\gamma_i$  correspond to  $z_i^{-1}$  in [14]. This reparametrization results in a swap of the hyperprior parameters  $a$  and  $b$ , and a change in the sign of  $c$  compared to [14, Table 1]. Furthermore, the Gamma hyperprior PDF corresponds to the inverse Gamma mixing distribution of [14, Table 1] and vice versa.

<sup>†</sup> While inverse Gamma hyperpriors are obtained for any  $c < 0$ , we consider only the case  $c = -\rho d_i - \frac{1}{2}$  since simplified updates exist for this case. For inverse Gamma distributions obtained by  $c \neq -\rho d_i - \frac{1}{2}$ , we refer the reader to the first row of this table.

through them and updating each estimate in turn with a revised estimate equal to the right-hand side of the corresponding equation in (12), or equivalently of the corresponding equation among (14), (15), or (18) with  $i = 1 \dots, K$  using the current estimates for all of the other factors. This iterative process is carried out until a convergence criterion is fulfilled. When we refer to this iterative algorithm we re-read the implicit equations (14), (15), or (18) with  $i = 1 \dots, K$  as updating equations where for each equation the estimate of the left-hand-side proximal PDF is updated according to the right-hand-side expression. We refer to this algorithm as variational BSBL (VA-BSBL).

### III. VARIATIONAL FAST SOLUTION

Using the VA-BSBL algorithm, the convergence of the mean-estimates  $\hat{\gamma}_i$  of the hyperparameters, given by (18), can be slow due to the cyclic dependency of  $\hat{\gamma}_i$  on  $\hat{\mathbf{x}}$  and  $\hat{\Sigma}$ , given by (15), and vice versa. To derive a fast-BSBL (F-BSBL) algorithm, we follow the approach of [5] and analyse repeated cycles of updates of  $q_{\mathbf{x}}$ , given by (15) and (18), respectively, followed by an update of the mean-estimate  $\hat{\gamma}_i$  of a single hyperparameter. Repeating this update-cycle *ad infinitum* yields a sequence of mean-estimates  $\{\hat{\gamma}_i^{[n]}\}_{n=1}^{\infty}$ . To accelerate convergence, we are interested in knowing if the sequence converges and, if it does converge, in its limit.

Note, that the parameter  $\hat{a}_i \triangleq \hat{a}_i(\hat{\gamma}_i)$  in (17) depends on the current estimate of  $\hat{\gamma}_i$  through the expectation  $\langle \mathbf{x}_i^H \mathbf{D}_i \mathbf{x}_i \rangle_{q_{\mathbf{x}}}$ , which is a function of the current estimate of  $\hat{\gamma}_i$  through (15). Therefore, updating  $q_{\mathbf{x}}$  using (15) followed by updating  $q_{\gamma_i}$  by inserting (17) into (18), the sequence of estimates  $\{\hat{\gamma}_i^{[n]}\}_{n=1}^{\infty}$  obtained by repeating this cycle can be viewed as generated by a first-order recurrence which maps from one estimate in the sequence to the next  $\hat{\gamma}_i^{[n+1]} = f_i(\hat{\gamma}_i^{[n]})$  using an update function  $f_i: \mathbb{R}_{++} \rightarrow \mathbb{R}_{++}$ , where

$$f_i(\gamma) = \sqrt{\frac{b}{\hat{a}_i(\gamma)}} \frac{K_{c_i+1}(\sqrt{b \hat{a}_i(\gamma)})}{K_{c_i}(\sqrt{b \hat{a}_i(\gamma)})}. \quad (19)$$

If the sequence of updates converges, the limit must be a fixed point  $\gamma^*$  of the recurrence relation, i.e. it must fulfill

$$f_i(\gamma^*) - \gamma^* = 0. \quad (20)$$

The following Lemmas 1 and 2 show that the expectation  $\langle \mathbf{x}_i^H \mathbf{D}_i \mathbf{x}_i \rangle_{q_{\mathbf{x}}}$ , and by extension  $\hat{a}_i(\hat{\gamma}_i)$ , is a strictly decreasing rational function of  $\hat{\gamma}_i$ . Lemma 3 and Corollary 1 show that  $f_i$  is strictly increasing. Thus, Theorem 1, a variant of the monotone convergence theorem [25, Theorem 3.14], can be used to determine under which condition the sequence  $\{\hat{\gamma}_i^{[n]}\}_{n=1}^{\infty}$  converges or diverges based on the set of fixed points of the update function  $f_i$ .

**Lemma 1.** *The term  $\langle \mathbf{x}_i^H \mathbf{D}_i \mathbf{x}_i \rangle_{q_{\mathbf{x}}}$  in (17) can be expressed as a rational function of the current estimate  $\hat{\gamma}_i$ , i.e.  $\langle \mathbf{x}_i^H \mathbf{D}_i \mathbf{x}_i \rangle_{q_{\mathbf{x}}} = B_i(\hat{\gamma}_i)/A_i(\hat{\gamma}_i)$ , where  $A_i(\gamma)$  and  $B_i(\gamma)$  are polynomials of degree  $2d_i$  and  $2d_i - 1$ , respectively, with positive coefficients.*

*Proof.* See Appendix A. ■

Note that by inserting  $\langle \mathbf{x}_i^H \mathbf{D}_i \mathbf{x}_i \rangle_{q_{\mathbf{x}}} = B_i(\hat{\gamma}_i)/A_i(\hat{\gamma}_i)$  from Lemma 1 into the simplified updates of  $\hat{\gamma}_i$  given in the third column of Table I, we obtain simplified expressions for the update function  $f_i$ , which are given in the fourth column of Table I. Moreover, by inserting these simplified expressions for the update function  $f_i$  into the fixed point equation (20), we find the fixed points  $\gamma^*$  as the roots of polynomials  $G_i(\gamma)$ , which are given in the fifth column of Table I.

**Lemma 2.** *The rational function  $B_i(\gamma)/A_i(\gamma)$  is strictly decreasing on its domain  $\mathbb{R}_{++}$ .*

*Proof.* See Appendix B. ■

**Lemma 3.** *The function  $h_{\alpha}(u) = u^{-1/2} K_{\alpha+1}(\sqrt{u})/K_{\alpha}(\sqrt{u})$  defined on  $\mathbb{R}_{++}$  is strictly decreasing for all  $\alpha \in \mathbb{R}$ .*

*Proof.* See Appendix C. ■

**Corollary 1.** *The update function  $f_i$  given in (19) is strictly increasing.*

*Proof.* Let  $u_i(\gamma) = b \hat{a}_i(\gamma) = b B_i(\gamma)/A_i(\gamma) + a b$ , such that (19) can be expressed as composition  $f_i(\gamma) = b h_{c_i} \circ u_i(\gamma)$ , where  $h_{c_i}(u)$  is the function defined in Lemma 3. Lemmas 2 and 3 show the functions  $h_{c_i}(u)$  and  $u_i(\gamma)$  to be strictly decreasing. Hence, their composition is strictly increasing. ■

**Theorem 1.** For any initial condition  $\hat{\gamma}_i^{[0]} > 0$ , the convergence of the sequence of estimates  $\{\hat{\gamma}_i^{[n]}\}_{n=1}^{\infty}$  generated by a first-order recurrence with function  $f_i$  in (19), is governed by the set  $\mathcal{G}_i = \{\gamma^* \in \mathbb{R}_{++} : f_i(\gamma^*) - \gamma^* = 0\}$  of fixed points as

$$\lim_{n \rightarrow \infty} \hat{\gamma}_i^{[n]} = \begin{cases} \infty & \text{if } f_i(\hat{\gamma}_i^{[0]}) > \hat{\gamma}_i^{[0]} \text{ and } \mathcal{G}_i^+ = \emptyset \\ \min \mathcal{G}_i^+ & \text{if } f_i(\hat{\gamma}_i^{[0]}) > \hat{\gamma}_i^{[0]} \text{ and } \mathcal{G}_i^+ \neq \emptyset \\ \max \mathcal{G}_i^- & \text{if } f_i(\hat{\gamma}_i^{[0]}) \leq \hat{\gamma}_i^{[0]} \end{cases} \quad (21)$$

where  $\mathcal{G}_i^+ = \{\gamma^* \in \mathcal{G}_i : \gamma^* > \hat{\gamma}_i^{[0]}\}$  is the subset of fixed points greater than the initial value  $\hat{\gamma}_i^{[0]}$ ,  $\mathcal{G}_i^- = \{\gamma^* \in \mathcal{G}_i : \gamma^* \leq \hat{\gamma}_i^{[0]}\}$  is the subset of fixed points smaller than or equal to the initial value  $\hat{\gamma}_i^{[0]}$ , and  $\emptyset$  denotes the empty set.

*Proof.* Since  $f_i$  is strictly increasing, the sequence  $\{\hat{\gamma}_i^{[n]}\}_{n=1}^{\infty}$  is either strictly increasing if  $f_i(\hat{\gamma}_i^{[0]}) > \hat{\gamma}_i^{[0]}$ , or strictly decreasing if  $f_i(\hat{\gamma}_i^{[0]}) < \hat{\gamma}_i^{[0]}$ , while the case  $f_i(\hat{\gamma}_i^{[0]}) = \hat{\gamma}_i^{[0]}$  is trivial. By definition every fixed point  $\gamma^* \in \mathcal{G}_i$  must fulfil  $f_i(\gamma^*) = \gamma^*$ . Since  $f_i$  is strictly increasing, it follows that the sequence  $\{\hat{\gamma}_i^{[n]}\}$  is upper bounded by  $\min \mathcal{G}_i^+$  (if such a fixed point exists) and lower bounded by  $\max \mathcal{G}_i^-$ . The monotone convergence theorem [25, Theorem 3.14] states, that the sequence  $\{\hat{\gamma}_i^{[n]}\}_{n=1}^{\infty}$  converges to the upper bound if it is increasing or to the lower bound if it is decreasing. If the sequence is decreasing, it cannot diverge since  $f_i$  is positive by definition. Thus, a fixed point  $\gamma^*$  must exist in the interval  $(0, \hat{\gamma}_i^{[0]})$  and, consequently,  $\mathcal{G}_i^-$  cannot be empty. If the sequence is increasing and no fixed point  $\gamma^*$  exists in the interval  $(\hat{\gamma}_i^{[0]}, \infty)$ , i.e. if  $\mathcal{G}_i^+$  is empty, we can always find some small constant  $\Delta : f_i(\hat{\gamma}_i^{[n]}) - \hat{\gamma}_i^{[n]} \geq \Delta > 0 \forall n \in \mathbb{N}$ . Hence, for any arbitrarily large positive constant  $C$  we find  $\hat{\gamma}_i^{[n]} > C \forall n > \lceil \frac{C}{\Delta} \rceil$ , i.e. the sequence diverges.<sup>4</sup> ■

Constraining ourselves to the special cases of the hyperprior  $p(\gamma)$  listed in the second row of Table I, we derive a fast update rule for  $q_{\gamma_i}$  and  $q_{\mathbf{x}}$  as follows. First, the set of fixed points  $\mathcal{G}_i$  is obtained by solving for the roots of the polynomial  $G_i(\gamma)$  (given in the fifth row of Table I), Next, we apply Theorem 1 and (21) to update our estimate of  $\hat{\gamma}_i$ . We use this fast update in a “fast” version of the VA-BSBL algorithm, referred to as F-BSBL.

*Discussion of Theorem 1:* While [5, Theorem 1] gives under which condition a (locally stable) fixed point exists, it is only applicable for the standard SBL case  $d_i = 1$ ,  $i = 1, \dots, K$ . In the block-sparse case, i.e.  $d_i > 1$  for some  $i = 1, \dots, K$ , several such fixed points might exist since the polynomial  $G_i(\gamma)$  can have up to  $P$  positive roots with  $P$  denoting its degree. To find the limit of the sequence  $\{\hat{\gamma}_i^{[n]}\}_{n=1}^{\infty}$  for  $d_i > 1$ , we need a method to determine to which of those fixed points

<sup>4</sup>We use  $\lceil \cdot \rceil$  to denote the operation of rounding up to the next highest integer number.

---

### Algorithm 1 F-BSBL

---

**Input:** Observations  $\mathbf{y}$ , dictionary  $\Phi$ , precision matrices  $\mathbf{D}_i$ .

**Output:** Weights  $\hat{\mathbf{x}}$ , hyperparameters  $\hat{\gamma}$ , noise precision  $\hat{\lambda}$ .

Initialize  $n = 1$ ,  $\hat{\lambda} = \frac{2N}{\|\mathbf{y}\|^2}$  and  $\hat{\gamma}_i = \infty$  for  $i = 1, \dots, K$ .

**while** not converged **do**

**for all** blocks  $i \in \{1, 2, \dots, K\}$  **do**

$\hat{\Sigma} \leftarrow (\hat{\lambda} \Phi^H \Phi + \sum_{k=1, k \neq i}^K \hat{\gamma}_k \mathbf{E}_k \mathbf{D}_k \mathbf{E}_k^T)^{-1}$ .

    Calculate  $\mathbf{U}_i$ ,  $\mathbf{S}_i$  and  $\mathbf{q}_i$  (See Appendix A).

    Obtain the roots of  $G_i(\gamma)$  in  $\mathbb{R}_{++}$ .

**if**  $n \leq 3$  **then**

      Update  $\hat{\gamma}_i$  using (21), assuming  $\hat{\gamma}_i^{[0]} = 0$ .

**else**

      Update  $\hat{\gamma}_i$  using (21).

**end if**

**end for**

$\hat{\Sigma} \leftarrow (\hat{\lambda} \Phi^H \Phi + \mathbf{D}_{\hat{\gamma}})^{-1}$ .

$\hat{\mathbf{x}} \leftarrow \hat{\lambda} \hat{\Sigma} \Phi^H \mathbf{y}$ .

  Update  $\hat{\lambda}$  using (14).

$n \leftarrow n + 1$ .

**end while**

---

the sequence converges. While no such a method is specified in [5, Theorem 1], (21) in our Theorem 1 allows to determine to which of the fixed points the sequence converges.

## IV. EFFICIENT IMPLEMENTATION

Note that all rows and columns of  $\hat{\Sigma}$  in (15) which correspond to a block  $i$  with  $\hat{\gamma}_i = \infty$  will be zero. Hence, the F-BSBL algorithm can be implemented efficiently by considering only the nonzero rows and columns of  $\hat{\Sigma}$ . As detailed in Algorithm 1,<sup>5</sup> we initialize the algorithm with  $\hat{\lambda} = 2N/\|\mathbf{y}\|^2$  and  $\hat{\gamma}_i = \infty \forall i$  (i.e. with an empty model).

We cycle through all blocks  $i \in \{1, 2, \dots, K\}$  to update  $\hat{\gamma}_i$  using the “fast” solution (21). We perform an update of the noise precision  $\hat{\lambda}$  after we updated all  $\hat{\gamma}_i$ . These steps are iterated until a convergence criterion is fulfilled. Using scaled Jeffrey’s prior with  $c > 0$ , the ELBO can be shown to diverge as  $\hat{\gamma}_i \rightarrow \infty$ , resulting in the trivial solution  $\hat{\gamma}_i = \infty \forall i$ . To avoid this trivial solution, we update  $\hat{\gamma}_i$  as if the previous value was  $\hat{\gamma}_i^{[0]} = 0$  in the first three iterations, which allows the estimate to converge to some local optimum at  $\hat{\gamma}_i < \infty$ . Note, that these modified updates of  $\hat{\gamma}_i$  might decrease the ELBO. Nevertheless, we perform such modified updates only in the first three iterations to achieve a better initialization. After the third iteration, we only perform unmodified updates, which are guaranteed to increase the ELBO. Therefore, the F-BSBL algorithm detailed in Algorithm 1 is guaranteed to converge to a (local) supremum of the ELBO.

*Computational Complexity:* Let  $\hat{M} = \|\hat{\mathbf{x}}\|_0$  denote the number of nonzero elements of  $\hat{\mathbf{x}}$ . Assuming that  $d_i$  is a small constant with respect to  $\hat{M}$ , the computational complexity for each step is as follows:

- Calculating the coefficients of the polynomials  $A_i(\gamma)$  and  $B_i(\gamma)$  is of complexity  $\mathcal{O}(\hat{M}^3)$ .

<sup>5</sup>Matlab code for the F-BSBL algorithm is available at <https://gitlab.com/jmoederl/fast-variational-block-sparse-bayesian-learning>

- Solving for the roots of the polynomial  $G_i(\gamma)$ , e.g. via the eigenvalues of the companion matrix [26], is of complexity  $\mathcal{O}(d_i^3)$ .
- Updating  $\hat{\gamma}_i$  according to Theorem 1 with  $\mathcal{G}_i$  already obtained is of complexity  $\mathcal{O}(d_i)$ .

The computationally most complex operation is the computation of the coefficients of  $A_i(\gamma)$  and  $B_i(\gamma)$ , since they require the inversion of the covariance matrix  $\hat{\Sigma}$ . Only rows and columns of  $\hat{\Sigma}$  corresponding to nonzero blocks ( $\hat{\gamma}_i < \infty$ ) must be considered. Hence, this operation is of complexity  $\mathcal{O}(\hat{M}^3)$ . Applying the EM-algorithm directly as in [13], the computationally most demanding operation is again the matrix inversion required for the covariance matrix. The EM-based algorithm [13] does not directly check for convergence. Thus,  $\hat{\gamma}_i = \infty$  is only achieved in the approximate sense, and only after many iterations. Therefore, the inversion of the covariance matrix must consider the full matrix, which is of complexity  $\mathcal{O}(N^3)$ . It follows from the sparsity assumption that  $\hat{M} \ll N$  and, thus, the F-BSBL algorithm is of lower computational complexity than the ones proposed in [13]. This difference is further enhanced by the fact that the fast update of  $\hat{\gamma}_i$  using Theorem 1 is the culmination of (infinitely) many individual updates. Hence, fewer iterations of the algorithms main-loop are required in the F-BSBL algorithm compared to EM-based algorithm in [13], as demonstrated in Section VII.

## V. ANALYSIS OF THE ALGORITHM

### A. Sparsity Inducing Selections of $a$ , $b$ and $c$

To perform sparse signal reconstruction and benefit from the computational efficiency gained by discarding blocks with weights  $x_i$  that are exactly zero, we are interested in hyper-priors  $p(\gamma; a, b, c)$  which result in a sparse estimate  $\hat{x}$  when applying Algorithm 1. However, a considerable range of values of  $a$ ,  $b$ , and  $c$  cannot result in a sparse estimate, as proven by the following Theorem 2.

**Lemma 4.** *The rational function defined in Lemma 1 behaves as  $B_i(\gamma)/A_i(\gamma) = d_i/\gamma + o(\gamma^{-2})$  as  $\gamma \rightarrow \infty$ .*

Here  $o(\cdot)$  is the little-o notation.

*Proof.* From (56) in Appendix B we obtain

$$\frac{B_i(\gamma)}{A_i(\gamma)} = \gamma^{-1} [d_i + o(1)\gamma^{-1}] \quad \text{as } \gamma \rightarrow \infty \quad (22)$$

after some algebraic manipulations.  $\blacksquare$

**Theorem 2.** *Setting either  $a > 0$  or  $c < 0$  is sufficient for the sequence  $\{\hat{\gamma}_i^{[n]}\}_{n=1}^{\infty}$  to converge.*

*Proof.* A sufficient condition for  $\{\hat{\gamma}_i^{[n]}\}_{n=1}^{\infty}$  to converge is that

$$f_i(\gamma) - \gamma < 0 \quad (23)$$

holds for any  $\gamma$  sufficiently large. Equation (23) is indeed sufficient for convergence, since  $f_i(\gamma) - \gamma$  is a continuous function and  $f_i(0) > 0$ . Thus, (23) implies the existence of at least one fixed point  $\gamma^*$ . The sequence  $\{\hat{\gamma}_i^{[n]}\}_{n=1}^{\infty}$  is guaranteed to converge by Theorem 1 for any initial value  $\hat{\gamma}_i^{[0]}$  smaller than the largest fixed point. Moreover, (23) implies that the

first iteration of  $f_i$  will be decreasing for any initial value  $\hat{\gamma}_i^{[0]}$  larger than the largest fixed point, which implies convergence by Theorem 1 as well.

*Case  $b > 0$  and  $a > 0$ :* Using Lemma 1 and (17), we write (19) as

$$f_i(\gamma) = b u_i(\gamma)^{-1/2} \frac{K_{c_i+1}(\sqrt{u_i(\gamma)})}{K_{c_i}(\sqrt{u_i(\gamma)})} \quad (24)$$

where  $u_i(\gamma) = b(a + 2\rho B_i(\gamma)/A_i(\gamma))$ . Applying Lemma 4, we find that  $u_i(\gamma)$  converges to  $ab > 0$  as  $\gamma \rightarrow \infty$ . Hence,  $f_i(\gamma)$  approaches some finite value as  $\gamma \rightarrow \infty$ , resulting in

$$\lim_{\gamma \rightarrow \infty} f_i(\gamma) - \gamma = -\infty < 0. \quad (25)$$

*Case  $b > 0$  and  $a = 0$ :* In this case,  $u_i(\gamma)$  converges to 0 as  $\gamma \rightarrow \infty$  by Lemma 4. From [27, Eq. (9.6.9)], we find that the function  $R_{c_i}(z) = K_{c_i+1}(z)/K_{c_i}(z)$  converges asymptotically to

$$\frac{K_{c_i+1}(z)}{K_{c_i}(z)} \sim \frac{2c_i}{z} \quad \text{as } z \rightarrow 0. \quad (26)$$

Let  $z = \sqrt{u_i(\gamma)}$ , we insert (26) into (24) and apply the definitions of  $A_i(\gamma)$  and  $B_i(\gamma)$  given in (53) and (54), respectively, to find

$$f_i(\gamma) - \gamma = \frac{c}{\rho d_i} \gamma + o(1) \quad \text{as } \gamma \rightarrow \infty \quad (27)$$

which fulfills the sufficient condition (23) if  $c < 0$ .

*Case  $b = 0$  and  $a > 0$ :* Using the simplified expression for  $f_i$  given in the third row of Table I, we find that

$$f_i(\gamma) - \gamma = -\gamma + o(1) \quad \text{as } \gamma \rightarrow \infty \quad (28)$$

after a few algebraic manipulations.

*Case  $b = 0$  and  $a = 0$ :* Using the definition of  $f_i$  given in the fourth row of Table I, we find

$$f_i(\gamma) - \gamma = \frac{c}{\rho d_i} \gamma + o(1) \quad \text{as } \gamma \rightarrow \infty \quad (29)$$

same as for the case  $b > 0$ .  $\blacksquare$

A sparse result is obtained if, and only if, the sequence of updates  $\{\hat{\gamma}_i^{[n]}\}_{n=1}^{\infty}$  diverges for some blocks  $i$ . Theorem 2 shows that the sequence of updates cannot diverge if either  $a > 0$  or  $c < 0$ , i.e. these parameter settings cannot result in a sparse estimate. Since we aim for a sparse estimate and the set of fixed points  $\mathcal{G}_i$  cannot be obtained in closed form for  $b > 0$ , we focus primarily on the case  $a = b = 0$  and  $c \geq 0$ , i.e. (scaled) Jeffrey's prior  $p(\gamma; c) \propto \gamma^{c-1}$ .

### B. Additional Thresholding

When utilizing SBL for line spectrum estimation—which includes the applications of arrival direction and arrival time estimation—it is known to overestimate the number of components [28]–[31]. A common solution to this problem is to introduce an additional thresholding operator that prunes away components for which little evidence exists in the data [30], [31]. For variational SBL, [5] suggested to introduce such a pruning as follows. In order to be a limit of the VB update

sequence, each fixed point  $\gamma^* \in \mathcal{G}_i$  must be locally stable. A fixed point  $\gamma^*$  is locally stable if, and only if [5]

$$|f'_i(\gamma)|_{\gamma=\gamma^*} < 1 \quad (30)$$

where  $(\cdot)'$  denotes the derivative. Reference [5] showed, that for  $d_i = 1$  and using Jeffrey's prior as hyperprior PDF  $p(\gamma_i)$ , the condition (30) equals  $\frac{q_{i,1}^2}{s_{i,1}} \geq 1$  and suggests to introduce a heuristic threshold  $\frac{q_{i,1}^2}{s_{i,1}} > \chi' \geq 1$  to increase the sparsity of the estimator. They verified the effectiveness of this method through numerical simulations. For  $d_i > 1$ , the relation between condition (30) and the values of  $q_{i,l}$  and  $s_{i,l}$ ,  $l \in \{1, 2, \dots, d_i\}$  is more involved. Nevertheless, we can apply the same intuition and heuristically introduce a threshold  $\chi \leq 1$ , such that each fixed point  $\gamma^*$  must fulfill

$$|f'_i(\gamma)|_{\gamma=\gamma^*} < \chi \quad (31)$$

in order to be considered as member of the sets of potential fixed points  $\mathcal{G}_i$  for the fast update rule. A disadvantage of this approach is that for  $\chi < 1$  the fast update might not correspond to the result of an infinite sequence of VB updates anymore. Hence, any guarantee that the ELBO is increased in each step and that the algorithm converges is lost.

Let us point out, for the scaled Jeffrey's PDF, increasing  $c$  results in the hyperprior PDF  $p(\gamma; c) \propto \gamma^{c-1}$  placing increasingly more probability mass on larger hyperparameters  $\gamma_i$ . Since the hyperparameters  $\gamma_i$  scale the prior precision matrix of each block, this can be interpreted as an additional force that drives the weight estimates towards  $\hat{x}_i = \mathbf{0}$ . Hence, the parameter  $c$  can be used to tune the desired (i.e. the a priori expected) sparsity of the estimator in a similar fashion as the heuristic threshold  $\chi$ . However, no modification of the update rules is required in this case. Therefore, the algorithm is still guaranteed to increase the ELBO in each step and, thus, guaranteed to converge. However, the ELBO diverges as  $\hat{\gamma}_i \rightarrow \infty$  if  $c > 0$  and  $a = 0$ , resulting in the trivial solution  $\hat{\gamma}_i = \infty \forall i$ . Nevertheless, using the updated schedule as described in Section IV, this trivial solution did not impact our numerical results, since the F-BSBL algorithm is only guaranteed to converge to a local optimum.

According to Theorem 2, priors parametrized with  $c = 0$  and  $b > 0$ , i.e. priors of the form  $p(\gamma; b) \propto \gamma^{-1} \exp\{-b/(2\gamma)\}$ , result in a sparse estimate and, since  $c = 0$ , the ELBO does not diverge as  $\hat{\gamma}_i \rightarrow \infty$ . Reference [32] shows that, when maximizing the marginal likelihood, the only prior which fulfills certain technical recovery conditions is  $p(\gamma; b) \propto \exp\{-b/\gamma\}$  with  $b \in \mathbb{R}_+$ . In the VB approach to SBL, Jeffrey's prior  $p(\gamma) \propto \gamma^{-1}$  is equivalent to a flat prior  $p(\gamma_i) = \text{const.}$  in the marginal likelihood approach. Thus, the prior  $p(\gamma; b) \propto \gamma^{-1} \exp\{-b/(2\gamma)\}$  obtained by  $a = c = 0$  seems to be the VB equivalent to the prior suggested by [32]. However, we consider a proof of their equivalence outside the scope of this work.

### C. Simulation Study

In order to verify the theoretical analysis of Section V-A and to investigate the heuristic approach of Section V-B, we

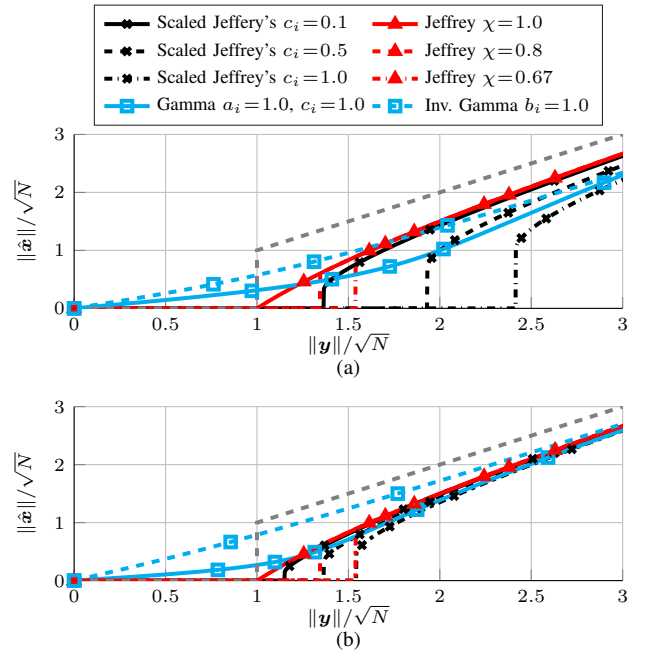


Fig. 1. Thresholding function for a system with an identity measurement matrix,  $\Phi = \mathbf{I}_N$ , consisting of a single block, i.e.  $K = 1$  and  $d_1 = N$  using different settings of the generalized inverse Gaussian prior. Subfigure (a) shows block size  $d_1 = N = 2$  and (b) block size  $d_1 = N = 10$ .

conduct the following experiment illustrating the thresholding behaviour depending on the chosen hyperprior  $p(\gamma)$ . A noiseless system is considered with an identity measurement matrix, i.e.  $M = N$  and  $\Phi = \mathbf{I}_N$ , consisting of a single block, i.e.  $K = 1$  and  $d_1 = N$ , resulting in the trivial model  $\mathbf{y} = \mathbf{x}$ . Since  $\Phi = \mathbf{I}_N$ , a perfect estimator for the noiseless case would be  $\hat{x} = \mathbf{y}$ . However, to obtain a sparse estimate in more practical scenarios, small values of  $\|\hat{x}\|$ , relative to the assumed/estimated noise variance  $1/\hat{\lambda}$ , should be thresholded by the estimator.

Let  $\mathbf{1}_N$  denote a vector of ones with length  $N$ , weights  $\mathbf{x} = \alpha \mathbf{1}_N$  and corresponding (noiseless) measurements  $\mathbf{y} = \mathbf{x}$  are generated repeatedly using different scales  $\alpha$ . We evaluate the fast update rule for  $\hat{\gamma}_1$  and the resulting weight estimate  $\hat{x}$  depending on the amplitude  $\alpha$  of  $\mathbf{x}$  for fixed  $\hat{\lambda} = 1$ . Figure 1a and 1b show the RMS amplitude  $\|\hat{x}\|/\sqrt{N}$  of the weights  $\hat{x}$ . ‘‘Hard’’ thresholding is given by  $\hat{x} = \mathbf{y}$  if  $\|\mathbf{y}\|/\sqrt{N} > 1$  and  $\hat{x} = \mathbf{0}$  otherwise. It is shown by the dashed gray lines in Figure 1.

Comparing the estimator obtained by different parameters of the generalized inverse Gaussian hyperprior PDF, it can be observed that the Gamma prior and the inverse Gamma prior do not show any thresholding, since  $\hat{x} = \mathbf{0}$  if and only if  $\mathbf{y} = \mathbf{0}$ . This is in line with both Theorem 2 and similar results from the literature [9], [14]. Comparing the scaled Jeffrey's prior and Jeffrey's prior, we see that, indeed, both estimators show a thresholding behavior since small (nonzero) values of  $\mathbf{y}$  lead to  $\hat{x} = \mathbf{0}$ . An increase in the threshold naturally results in a higher degree of sparsity in the estimate in more complex scenarios. Furthermore, it is noteworthy to highlight the effect of different block sizes on the solution ( $d_i = 2$  and  $d_i = 10$

shown in Figure 1a and 1b, respectively). The cutoff value for Jeffery's prior remains constant even with different thresholds, relative to the average amplitude of the components within the block. However, the likelihood of the average component amplitude being high decreases as the block size increases, due to the low likelihood of all amplitudes being high in the same realization. Consequently, a fixed threshold  $\chi$  would result in varying false alarm rates depending on the block size. In contrast, using a scaled Jeffrey's prior leads to a reduction of the cutoff region with an increase in block size, compensating to some extent for the reduction of the false alarm rate.

Finally, from Figure 1 we can see that with  $c$  and  $\chi$  tuned to achieve a similar thresholding (e.g.  $c = 1$  and  $\chi = 0.67$  for a block size of  $d_i = 10$ ), the estimation performance of both estimators is rather similar. To retain the convergence guarantees of the VB algorithm, we conclude that the scaled Jeffrey's prior is to be preferred over Jeffrey's prior with an additional threshold.

## VI. EQUIVALENCE BETWEEN BSBL VARIANTS

Reference [16] showed the equivalence between SBL based on the EM algorithm and VB inference for the classical model with independent weights. In this section, we generalize the result from [16] to the block-sparse case. Our Theorem 3 unifies the EM-based Type-II-BSBL, e.g. [12], [13], and the VA-BSBL presented in this work, under a common mathematical framework. To do so, we first generalize [16, Theorem 1] to the case of multivariate  $p(\mathbf{x})$ .

**Lemma 5.** *A multivariate PDF  $p(\mathbf{x}) = h \circ z(\mathbf{x})$ , where  $h(z) = \exp(-g(z^2))$  and  $z(\mathbf{x}) = \sqrt{\mathbf{x}^H \mathbf{D} \mathbf{x}}$  with some positive-definite matrix  $\mathbf{D}$ , can be represented in the convex variational form*

$$p(\mathbf{x}) \propto \sup_{\gamma > 0} \mathcal{N}(\mathbf{x}; \mathbf{0}, (\gamma \mathbf{D})^{-1}) \varphi(\gamma) \quad (32)$$

if, and only if,  $g(z)$  is non-decreasing and concave on  $(0, \infty)$ . In this case, we can use the function

$$\varphi(\gamma) = |(\rho\gamma/\pi)\mathbf{D}|^{-\rho} \exp(g^*(\rho\gamma)) \quad (33)$$

where  $g^*$  is the concave conjugate of  $g$ .

*Proof.* Applying [16, Theorem 1] to  $h(z)$  yields

$$h(z) = \sup_{\xi > 0} \mathcal{N}(z; 0, \xi^{-1}) \sqrt{2\pi/\xi} \exp(g^*(2\xi)). \quad (34)$$

Inserting (34) into the composition  $p(\mathbf{x}) = h \circ z(\mathbf{x})$  yields (32) after substituting  $\xi = 2\rho\gamma$  and some algebraic manipulations. ■

Let  $p(\mathbf{x}) = \prod_{i=1}^K p(\mathbf{x}_i)$  be a product of independent identical prior PDFs  $p(\mathbf{x}_i)$ , each of which admits the convex variational representation (32). By omitting the maximization over the variational parameter  $\gamma_i$  of each prior PDF  $p(\mathbf{x}_i)$ ,  $i = 1, \dots, K$ , we obtain a lower bound on the evidence  $p(\mathbf{y}) = \int p(\mathbf{y}|\mathbf{x})p(\mathbf{x})d\mathbf{x}$  as

$$p(\mathbf{y}) \geq \int p(\mathbf{y}|\mathbf{x}) \prod_{i=1}^K p(\mathbf{x}_i; \gamma_i) \varphi(\gamma_i) d\mathbf{x} \triangleq \tilde{p}(\mathbf{y}; \boldsymbol{\gamma}) \quad (35)$$

which is parameterized by  $\boldsymbol{\gamma} = [\gamma_1 \ \gamma_2 \ \dots \ \gamma_K]^T$ , where  $p(\mathbf{x}_i; \gamma_i) = \mathcal{N}(\mathbf{x}_i; \mathbf{0}, (\gamma_i \mathbf{D}_i)^{-1})$ . Note, that for  $\varphi(\gamma) = \text{const.}$ , the function  $\tilde{p}(\mathbf{y}; \boldsymbol{\gamma})$  corresponds to the marginal likelihood that is maximized, e.g. in the EM-based Type-II-BSBL [13] and the fast Type-II-BSBL [11].

The EM approach obtains estimates  $\hat{\boldsymbol{\gamma}}_{\text{EM}}$  of the parameters  $\boldsymbol{\gamma}$  by iteratively maximizing the function

$$Q(\boldsymbol{\gamma}, q_{\text{EM}}(\mathbf{x})) = \left\langle \ln \frac{p(\mathbf{y}|\mathbf{x}) \prod_{i=1}^K p(\mathbf{x}_i; \gamma_i) \varphi(\gamma_i)}{q_{\text{EM}}(\mathbf{x})} \right\rangle_{q_{\text{EM}}(\mathbf{x})} \quad (36)$$

with respect to  $\boldsymbol{\gamma}$  and the distribution  $q_{\text{EM}}$ . The following Theorem 3 proves the equivalency between the EM and VB approaches to BSBL, in case  $p(\boldsymbol{\gamma})$  and  $\varphi(\boldsymbol{\gamma})$  are chosen such that they result in the same prior  $p(\mathbf{x}_i)$  according to (5) and (32), respectively.

**Theorem 3.** *The distribution  $q_{\text{EM}}$  maximizing (36) is equal to  $q_{\mathbf{x}}$  obtained from (12) if, and only if, the estimates  $\hat{\boldsymbol{\gamma}}_{\text{EM}}$  and  $\hat{\boldsymbol{\gamma}}$  for the EM and VB algorithm, respectively, are equal. Similarly, the updates of single elements of  $\hat{\boldsymbol{\gamma}}_{\text{EM}}$  and  $\hat{\boldsymbol{\gamma}}$  for the EM and VB algorithm, respectively, are identical if  $q_{\mathbf{x}} = q_{\text{EM}}$ . In that case,*

$$\hat{\gamma}_{i,\text{EM}} = \hat{\gamma}_i = h'_i(u_i(q_{\mathbf{x}})) \quad (37)$$

where  $h'_i(u_i)$  is the first derivative of some function  $h_i(u_i)$  and  $u_i = u_i(q_{\mathbf{x}}) = \rho \langle \mathbf{x}_i^H \mathbf{D}_i \mathbf{x}_i \rangle_{q_{\mathbf{x}}(\mathbf{x})}$ .

*Proof.* It is straightforward to show that the distribution  $q_{\text{EM}}$  obtain by maximizing the function  $Q(\boldsymbol{\gamma}, q_{\text{EM}})$  for fixed  $\boldsymbol{\gamma} = \hat{\boldsymbol{\gamma}}$  is equal to the distribution  $q_{\mathbf{x}}$  obtained by the VA-BSBL algorithm described in Section II-C. The proof of (37), i.e. the proof of equivalence of the updates of  $\hat{\gamma}_i$ , is found in Appendix E. ■

**Corollary 2.** *The elements of the set*

$$\{\boldsymbol{\gamma}^* \in \mathbb{R}_{++} : f_i(\boldsymbol{\gamma}^*) - \boldsymbol{\gamma}^* = 0, |f'_i(\boldsymbol{\gamma})|_{\boldsymbol{\gamma}=\boldsymbol{\gamma}^*} < 1\} \quad (38)$$

i.e. the stable fixed points of the fast VB update, are local maxima of  $\tilde{p}(\mathbf{y}; \tilde{\boldsymbol{\gamma}}_i)$  with respect to a single entry  $\gamma_i$ , where  $\tilde{\boldsymbol{\gamma}}_i = [\hat{\gamma}_1 \ \hat{\gamma}_2 \ \dots \ \hat{\gamma}_{i-1} \ \gamma_i \ \hat{\gamma}_{i+1} \ \dots \ \hat{\gamma}_K]^T$ .

*Proof.* The EM updates of  $q_{\text{EM}}$  and  $\hat{\boldsymbol{\gamma}}_{i,\text{EM}}$  are guaranteed to increase the value of  $\tilde{p}(\mathbf{y}; \boldsymbol{\gamma})$  evaluated at  $\boldsymbol{\gamma} = \hat{\boldsymbol{\gamma}}_{\text{EM}}$ . Theorem 3 proves that the EM and VB updates of  $\hat{\boldsymbol{\gamma}}$  are equivalent. Hence, each VB updated according to (12) increases the value of  $p(\mathbf{y}; \hat{\boldsymbol{\gamma}})$  and so does each step in the update sequence  $\{\hat{\gamma}_i^{[n]}\}_{n=1}^{\infty}$ . Consequently, a necessary condition for  $\lim_{n \rightarrow \infty} \hat{\gamma}_i^{[n]} = \gamma_i$  is that  $\gamma_i$  is a local maximum of  $p(\mathbf{y}; \tilde{\boldsymbol{\gamma}}_i)$ . ■

As shown in Appendix D, the prior  $p(\mathbf{x}_i)$  in (8) used in this work admits the convex representation (32). Thus, Theorem 3 and Corollary 2 show that (i) EM-based Type-II-BSBL is equivalent to the VA-BSBL algorithm, and (ii) also their fast variants, i.e. the fast Type-II-BSBL using coordinate ascent for the former, e.g. [11], and F-BSBL for the latter, are equivalent. As a result of (i), the presented fast solution can also be applied to [13] and similar EM-based Type-II-BSBL algorithms. Note, that the integral representation (5)

of  $p(\mathbf{x}_i)$  using Jeffrey's prior  $p(\gamma) \propto \gamma^{-1}$  can be shown to correspond to  $\varphi(\gamma) = \text{const.}$  in the convex representation (32) of  $p(\mathbf{x}_i)$ . Thus, the resulting EM and VB updates must be identical according to Theorem 3. Indeed, the update rule of the EM-based Type-II-BSBL algorithm [13] is equivalent to update rule  $\hat{\gamma}_i = d_i / \langle \mathbf{x}_i^H \mathbf{D}_i \mathbf{x}_i \rangle_{q_{\mathbf{x}_i}}$  of the VA-BSBL algorithm using Jeffrey's prior.<sup>6</sup> Furthermore, an illustrative example of Corollary 2 is given in Appendix F, which explicitly details the equivalence between the implementation of fast Type-II-F-BSBL using coordinate ascent of [11] and the presented F-BSBL algorithm using Jeffrey's prior.

## VII. NUMERICAL EVALUATION

To investigate the performance of the algorithm, we generate an dictionary matrix with  $M = 2N$  columns and assume  $N = 200$  measurements are obtained unless otherwise stated. The elements of the dictionary matrix are drawn from independent zero-mean normal distributions with unit variance and each column  $\phi_k$  of  $\Phi$  is normalized such that  $\|\phi_k\| = 1$ . The the corresponding weight vector  $\mathbf{x}$  is partitioned into blocks with an equal block size of  $d_i = 10 \forall i$ . We selected a number of blocks at randomly chosen locations such that the desired sparsity ratio  $\delta = \frac{\|\mathbf{x}\|_0}{N} = 0.2$  was achieved. For these nonzero blocks we draw  $\mathbf{x}_i$  from a Gaussian distribution with zero mean and unit variance while for the remaining blocks  $\mathbf{x}_i = 0$ . The location of the nonzero blocks is unknown to the algorithm. The noise precision  $\lambda$  is chosen, such that the signal-to-noise ratio (SNR) defined as  $\text{SNR} = \frac{\lambda \|\Phi \mathbf{x}\|^2}{N}$  equals 15 dB. As performance metric we use the normalized mean squared error (NMSE) defined as  $\text{NMSE} = \frac{\|\mathbf{x} - \hat{\mathbf{x}}\|^2}{\|\mathbf{x}\|^2}$ , averaged over 100 simulation runs. We use Jeffrey's prior for the noise precision  $p(\lambda)$ , which is obtained by  $\epsilon = \eta = 0$  in (9). Two variants of the F-BSBL algorithm are evaluated. Once using a Jeffrey's prior, obtained by  $a = b = c = 0$  in (6), as hyperprior  $p(\gamma)$  and a threshold of  $\chi = 0.67$ , and once using the scaled Jeffrey's prior with  $c = 1$  as hyperprior  $p(\gamma)$ . Since we are interested in sparse estimators, we did not consider the non-sparse variants of the hyperprior. As comparison methods we use two variants of the EM-based Type-II-BSBL algorithm from [13].<sup>7</sup> The comparison algorithms apply the EM algorithm directly (BSBL-EM) or use a bounded-optimization approach to increase the convergence speed of the EM algorithm (BSBL-BO). Note, that through the equivalence shown in Theorem 3, the BSBL-EM algorithm is equivalent to the VA-BSBL presented herein using Jeffrey's prior as hyperprior. For all algorithms we assumed that  $\mathbf{D}_i = \mathbf{I}$  is a known and fixed parameter. As reference, we also include an "oracle" minimum mean squared error (MMSE) estimator, which is given the true locations of the nonzero blocks and calculates the weights of the nonzero blocks using the pseudoinverse of the corresponding columns of the dictionary. The same convergence criterion is

<sup>6</sup>Reference [13] uses prior variances in their model instead of the prior precisions we use throughout the paper. Thus, the variable  $\hat{\gamma}_i$  in our derivations corresponds to  $\gamma_i^{-1}$  in [13].

<sup>7</sup>The code for the BSBL-EM and BSBL-BO algorithms was obtained from <http://dsp.ucsd.edu/~zhilin/BSBL.html>

used for all algorithms. Let  $\hat{\sigma} = [\hat{\gamma}_1^{-1} \hat{\gamma}_2^{-1} \dots \hat{\gamma}_K^{-1}]^T$  be a vector of the estimated prior variances. We considered each algorithm converged if the number and position of the nonzero blocks did not change from one iteration to the next and  $\|\hat{\sigma}^{[n]} - \hat{\sigma}^{[n-1]}\|_1 / \|\hat{\sigma}^{[n]}\|_1 < 10^{-4}$ , where  $\hat{\sigma}^{[n]}$  is the value of  $\hat{\sigma}$  estimated at the  $n$ th iteration, and  $\|\cdot\|_1$  denotes the  $\ell_1$ -norm.

Figures 2a-2c depict the NMSE of the algorithms as a function of the signal length  $N$ , the SNR and number of iterations. We define the number of iterations as the number of times the main loop of the algorithm is repeated, i.e. the amount of times all variables  $\hat{\mathbf{x}}$ ,  $\hat{\Sigma}$ ,  $\hat{\lambda}$  and  $\hat{\gamma}_1 \dots \hat{\gamma}_K$  are updated. Figure 2d shows the runtime of the algorithms again as function of the signal length  $N$ . For  $N = 500$ , the runtime of the F-BSBL algorithm is approximately 2 orders of magnitude smaller than that of the BSBL-EM and BSBL-BO algorithms [13], while achieving an NMSE virtually identical to that of the oracle MMSE estimator. As shown in Figures 2b and 2c, the F-BSBL algorithm achieves an NMSE almost identical to that of the oracle estimator already after 3 iterations and over a wide range of SNRs. Figure 2e shows the empirical probability of correctly estimating any  $\hat{\gamma}_i$  as converged or diverged (i.e. the empirical probability of classifying each block correctly as zero or nonzero block). While the F-BSBL algorithm classifies the blocks correctly as zero or nonzero almost all the time, the BSBL-EM and BSBL-BO algorithms overestimates the number of nonzero blocks (see Figure 2f). The false alarms of estimating some blocks  $\hat{\mathbf{x}}_i$  as nonzero even though the true weights  $\mathbf{x}_i$  used to generate the data are zero also leads to an increased NMSE of the BSBL-EM and BSBL-BO algorithms compared to the F-BSBL algorithm, as seen e.g. in Figure 2a.

The difference in the runtime of the algorithms can be explained by Figures 2c and 2f. While the F-BSBL algorithm achieves an NMSE estimate virtually identical to that of the oracle estimator after three iterations already, the BSBL-BO and BSBL-EM algorithms require far more iterations to converge. Furthermore, as detailed in Figure 2f, the F-BSBL algorithm estimates the number of active blocks correctly from the first iteration on. Thus, any operations that require the covariance of the weights  $\hat{\Sigma}$  can be performed with a small matrix since the entries of  $\hat{\Sigma}$  corresponding to deactivated blocks are exactly zero. It can be seen in Figure 2f, that the BSBL-BO algorithm keeps all 40 blocks active for the first 10 iterations and then slowly starts to deactivate blocks. The BSBL-EM algorithm keeps all 40 blocks active for the first 100 iterations before it starts to deactivate them. Thus, in addition to requiring more iterations until the convergence criterion is fulfilled, each iteration also involves operations with a larger matrix  $\hat{\Sigma}$ . Therefore, each iteration of BSBL-EM and BSBL-BO algorithms is computationally more expensive compared to the proposed algorithm.

Additionally, we evaluate how varying the block size  $d_i$  and the sparsity ratio  $\delta$  affects the algorithm performance in terms of NMSE. To evaluate the performance of the algorithm as function of the block size  $d_i$ , we use  $N = 500$  while we use  $N = 200$  for the evaluation over the sparsity ratio  $\delta$ . Figures 2g and 2h show the NMSE obtained by these numerical experiments. Again, the F-BSBL algorithm outperforms the

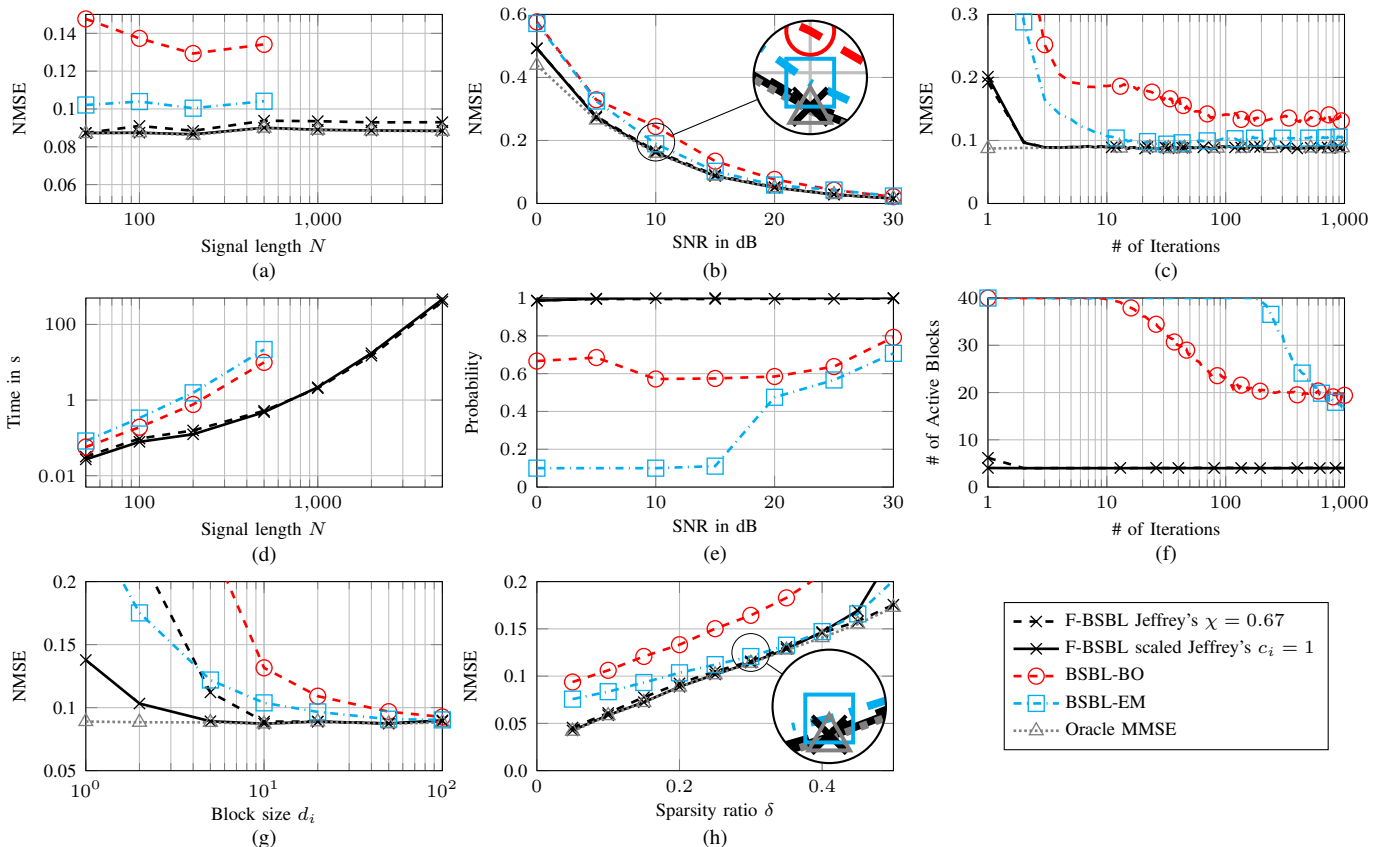


Fig. 2. Performance of the F-BSBL algorithm using a dictionary matrix with Gaussian distributed entries averaged over 100 realizations. NMSE as function of the signal length (a), SNR (b) and the number of iterations (c). The runtime of each algorithm as a function of the signal length is shown in (d). Classification probability of correctly classifying each block as zero/nonzero as a function of the SNR (e) and the number of active blocks ( $\hat{\mathbf{x}}_i \neq \mathbf{0}$ ) as function of the number of iterations (f). Further evaluation of the NMSE over block size (g) and sparsity ratio (h). Unless otherwise stated, the following parameters were used in the simulations.  $N = 200$ ,  $M = 2N$ , SNR = 15 dB,  $\delta = 0.2$  and  $d_i = 10 \forall i$ .

BSBL-EM and BSBL-BO algorithms over most simulated sparsity ratios and SNRs. An evaluation of the runtime and zero/nonzero classification probability was evaluated as well. However we found these results to be similar to the ones in Figure 2d and 2e. Thus, they are omitted for the sake of brevity. In case the block size is varied, F-BSBL with scaled Jeffrey's prior with  $c = 1$  is again superior to BSBL-EM and BSBL-BO, as well as to F-BSBL with Jeffrey's prior and a threshold of  $\chi = 0.67$ . The difference between the two variants of the F-BSBL algorithm stems from the dependence of the probability of missed detection and false alarms on the block size, which is more severe for Jeffrey's prior compared to the scaled Jeffrey's prior as discussed in Section V-C.

## VIII. APPLICATION EXAMPLE: DOA ESTIMATION

### A. System Model

Consider an unknown number of  $L$  narrowband sources with complex signal amplitudes  $s_l[t] \in \mathbb{C}$ ,  $l = 1, \dots, L$  located at fixed DOAs  $\theta_l \in \Theta = [-90^\circ, 90^\circ)$  in the far field of an array consisting of  $N$  sensors, such as a microphone or antenna array. Multiple measurements  $\mathbf{y}_t \in \mathbb{C}^N$  at different times  $t =$

$1, 2, \dots, d$  are obtained. Each measurement is modeled as

$$\mathbf{y}_t = \sum_{l=1}^L \psi(\theta_l) s_l[t] + \mathbf{v}_t \quad (39)$$

where  $\psi(\theta_l)$  is the steering vector of the array and  $\mathbf{v}_t$  is additive noise. We assume that the noise  $\mathbf{v}_t$  follows a Gaussian PDF  $\mathcal{N}(\mathbf{v}_t; \mathbf{0}, \lambda^{-1} \mathbf{I})$  and is independent across different times  $t$ . For a linear array, the steering vector is

$$\psi(\theta_l) = \frac{1}{\sqrt{N}} [1 \ e^{-j2\pi \frac{p_2}{\mu} \sin \theta_l} \ \dots \ e^{-j2\pi \frac{p_N}{\mu} \sin \theta_l}]^T \quad (40)$$

where  $\mu$  is the wavelength of the signal and  $p_n$  is the distance from sensor 1 to sensor  $n$ .

An alternative model can be obtained by introducing a search grid of  $K$  potential source DOAs  $\bar{\boldsymbol{\theta}} = [\bar{\theta}_1 \ \bar{\theta}_2 \ \dots \ \bar{\theta}_K]^T$  and corresponding amplitude vectors  $\mathbf{x}^{(t)}$ . With this grid we construct a dictionary matrix  $\Psi = [\psi(\bar{\theta}_1) \ \psi(\bar{\theta}_2) \ \dots \ \psi(\bar{\theta}_K)]$ , such that we approximate (39) as

$$\mathbf{y}_t = \Psi \mathbf{x}^{(t)} + \mathbf{v}_t. \quad (41)$$

Instead of directly estimating  $L$  and the DOAs  $\theta_1$  through  $\theta_L$  we obtain a sparse estimate of  $\mathbf{x}^{(t)}$  and use the number of nonzero elements of  $\mathbf{x}^{(t)}$  as estimate  $\hat{L}$  of  $L$ . From the

columns of  $\Psi$  corresponding to the active entries in  $\mathbf{x}^{(t)}$ , we can extract DOAs estimates  $\hat{\theta}_l$ ,  $l = 1, \dots, \hat{L}$ .

The locations of the sources are assumed stationary. Therefore, the sparsity profile of  $\mathbf{x}^{(t)}$  at different times  $t$  stays constant. Let  $\mathbf{Y} = [\mathbf{y}_1 \ \mathbf{y}_2 \ \dots \ \mathbf{y}_d]$ ,  $\mathbf{X} = [\mathbf{x}^{(1)} \ \mathbf{x}^{(2)} \ \dots \ \mathbf{x}^{(d)}]$  and  $\mathbf{V} = [\mathbf{v}_1 \ \mathbf{v}_2 \ \dots \ \mathbf{v}_d]$ , we arrive at the row-sparse MMV signal model

$$\mathbf{Y} = \Psi \mathbf{X} + \mathbf{V}. \quad (42)$$

As discussed in Section II-A, (42) can be rearranged into a block-sparse model. Thus, the row-sparse matrix  $\mathbf{X}$  can be estimated using the presented algorithm.

Note, that in this model the weights in each row of  $\mathbf{X}$ , (i.e. each block  $\mathbf{x}_i$  of  $\mathbf{x}$ ) are either zero or correspond to the amplitudes of a source over time  $\mathbf{x}_i = [s_i[1] \ s_i[2] \ \dots \ s_i[d]]^T$ . Thus, any prior knowledge about these source amplitudes can be incorporated in the matrix  $\mathbf{D}_i$ .

### B. DOA Estimation Results

Since the BSBL-EM and BSBL-BO algorithms from [13] are not applicable for a complex valued signal model, we compare the F-BSBL algorithm against the multi-snapshot DOA-SBL algorithm [19].<sup>8</sup> In this case, the actual weights  $\mathbf{X}$  are of secondary interest. Thus, we resort to the optimal subpattern assignment (OSPA) metric [33] of the estimated DOAs  $\hat{\theta}_l$ ,  $l \in \{1, \dots, \hat{L}\}$  to evaluate the performance of the algorithms. The OSPA is a metric which considers both the actual estimation error as well as the error in estimating the model order (i.e. the number of missed detection and false alarms). As parameters for the OSPA, we set the order to 1 and use a cutoff-distance of  $5^\circ$ . Since the DOA-SBL algorithm does not directly estimating a sparse weight vector, we evaluate two versions of this algorithm. Let  $\gamma_{i,\text{DOA-SBL}}$  and  $\sigma_{\text{DOA-SBL}}^2$  denote the prior variances and noise variance estimated by [19]. We define the component SNR of the  $i$ -th block as  $\text{SNR}_{i,\text{DOA-SBL}} = \frac{\gamma_{i,\text{DOA-SBL}}}{\sigma_{\text{DOA-SBL}}^2}$ . We consider all DOAs  $\hat{\theta}_i$  which have an associated component SNR above a certain threshold as first variant of the DOA-SBL algorithm.<sup>9</sup> Based on preliminary simulations, we adapted the threshold to maximize the performance of the DOA-SBL algorithm in our simulated scenarios. As an additional comparison, we also consider an oracle variant of the algorithm which is given the true number of components  $L$  and estimates  $\hat{\theta}_l$  as the DOAs corresponding to the  $L$  blocks with largest component SNR. To account for the increasing processing gain at increasing arrays sizes, we define the array SNR as for snapshot  $t$  as  $\text{SNR}_A = \lambda \|\Psi \mathbf{x}^{(t)}\|^2$ .

*Single-Snapshot Estimation Performance:* For the first experiment, we analyse the runtime and estimation accuracy as a function of the number of array elements  $N$ . We generate a dictionary with  $M = 2N$  entries spaced such that  $\sin(\hat{\theta}_m)$

<sup>8</sup>The code for the DOA-SBL algorithm was obtained from <https://github.com/gerstoft/SBL>.

<sup>9</sup>The authors of the DOA-SBL algorithm used a similar thresholding based on the maximum estimated prior variance  $\gamma_{i,\text{DOA-SBL}}$  in a related paper [34]. However, additional simulations which are omitted for brevity show that our thresholding based on the component SNR achieves a smaller OSPA than the method used in [34].

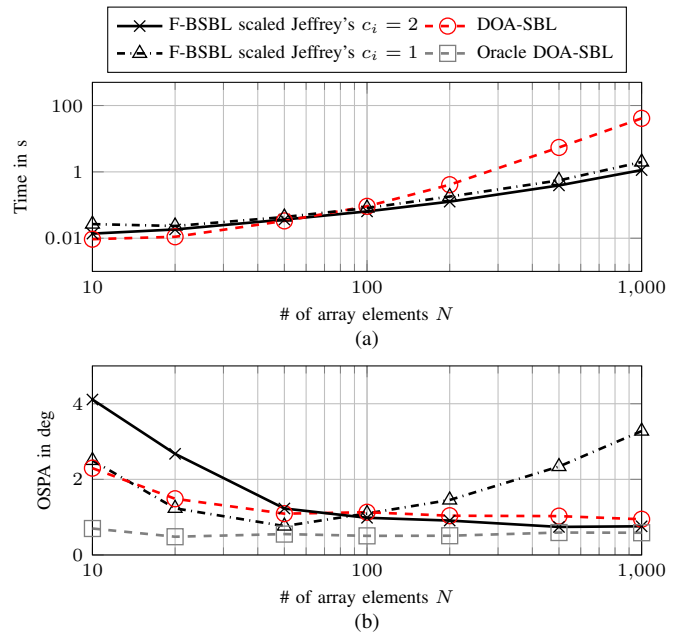


Fig. 3. Runtime (a) and OSPA (b) as function of the number of array elements at an  $\text{SNR}_A = 10$  dB for the F-BSBL algorithm compared to the DOA-SBL algorithm [19].

forms a regular grid. We simulate 3 sources located at the grid points closest to  $\{-2^\circ, 3^\circ, 50^\circ\}$  with amplitudes drawn randomly from a zero-mean complex Gaussian distribution with unit variance and consider only a single snapshot  $d = 1$ . For the DOA-SBL algorithm, we calculate the OSPA based on all blocks with component  $\text{SNR} \geq 10$  dB. To illustrate the effect of the parameter  $c$ , we use two variants of the F-BSBL algorithm. Both use the scaled Jeffrey's priors and are parameterized with  $c = 1$  and  $c = 2$ , respectively. Figures 3a and 3b show the runtime and OSPA, respectively, for both algorithms at an  $\text{SNR}_A = 20$  dB. The smallest OSPA is achieved by the oracle DOA-SBL algorithm. This is not surprising, since this algorithm is given the true number of sources in advance. However, knowing the true number of sources is not a realistic assumption for most practical applications. For array sizes of 100 elements and larger, the F-BSBL algorithm parameterized with  $c = 2$  is faster than the DOA-SBL algorithm while achieving the same OSPA. For array sizes with less than 100 elements, the OSPA for the F-BSBL algorithm parameterized with  $c = 2$  increases rapidly. This is due to some components not being detected in those cases. The parameter  $c$  acts similar to a threshold. Hence, we can increase the detection probability by using a smaller value for  $c$ . Consequently, this also leads to an increased false alarm rate. The increased false alarm rate is mostly noticeable at large  $N$ , due to the larger number of possible DOAs in the grid for large  $N$ . Hence, by using a smaller  $c$ , e.g.  $c = 1$ , we can reduce the OSPA at smaller array sizes at the cost of increasing the OSPA at larger array sizes, as shown in Figure 3b. We refer the reader to [30] for a detailed discussion on the relation between the array size and number of false alarms for a similar SBL-based approach.

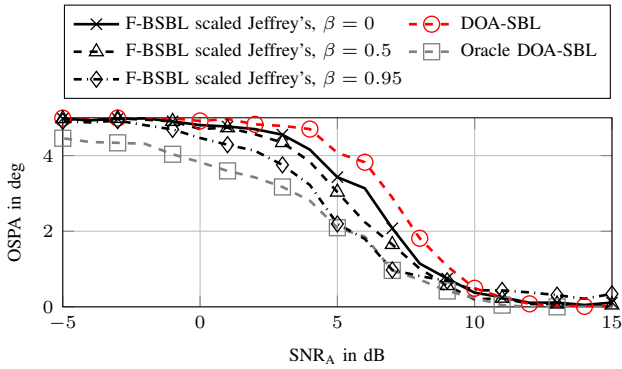


Fig. 4. OSPA of the F-BSBL algorithm and the DOA-SBL algorithm [19] as function of the  $\text{SNR}_A$  given  $d = 10$  snapshots with different source correlations  $\beta$ .

**Multi-Snapshot Estimation Performance:** Next, we simulate a system with an array consisting of  $N = 100$  antennas where  $d = 10$  snapshots are obtained. We simulate three sources at the same DOAs as in the previous experiment. To investigate the effect of intra-block correlations, the source amplitudes  $s_k[t]$  are generated by a first-order autoregressive model, i.e.  $s_k[t] = \xi + \beta s_k[t-1]$  where  $\xi \sim \text{CN}(\xi; 0, 1)$  is a circularly-symmetric zero-mean complex Gaussian random variable with unit variance. The coefficient  $\beta \in \mathbb{C} : |\beta| < 1$  can be used to set the correlation between the snapshots over time. The covariance matrix  $\Sigma_s$  of the samples  $s_k[t]$  is given as a Toeplitz matrix

$$\Sigma_s = \begin{bmatrix} 1 & \beta & \dots & \beta^{d-1} \\ \beta & 1 & \dots & \beta^{d-2} \\ \vdots & \vdots & \ddots & \vdots \\ \beta^{d-1} & \beta^{d-2} & \dots & 1 \end{bmatrix}. \quad (43)$$

We evaluate three different cases. (i) no correlation  $\beta = 0$ , (ii) medium correlation  $\beta = 0.5$  and (iii) strong correlation  $\beta = 0.95$ . For the F-BSBL algorithm we set  $D_i = \Sigma_s^{-1} \forall i$  to exploit this information. The correlation between the source amplitudes provides additional statistical information which can be used to separate true sources from the additive white noise. Therefore, the probability of false alarms gets smaller with increasing correlation  $\beta$ . To achieve an (approximately) constant false alarm rate for the F-BSBL algorithm, we parameterize the scaled Jeffrey's prior with  $c = 2$  for the case of no correlation (i) and medium correlation (ii), and use  $c = 1.5$  for high correlation (iii), based on preliminary simulations. For the DOA-SBL algorithm, we calculate the OSPA based on all blocks with a component  $\text{SNR} \geq 2$  dB, based on the same preliminary simulations. The performance of the DOA-SBL algorithm is approximately the same in all three cases, since it cannot exploit the additional information resulting from the correlation of the source amplitudes. Thus, we plot the performance of the DOA-SBL only for case (i). Figure 4 depicts the OSPA of both algorithms as a function of the  $\text{SNR}_A$ . For  $\text{SNR}_A < 0$  dB and  $\text{SNR}_A > 10$  dB, the estimation either fails due to the high noise level or is trivial. Thus the performance of both algorithms is approximately the same in these regions. In the transition region  $0 \text{ dB} \leq \text{SNR}_A \leq 10 \text{ dB}$ ,

the F-BSBL algorithm achieves a smaller OSPA than the DOA-SBL algorithm for all three cases. With increasing correlation, the performance of the F-BSBL algorithm improves. For the case of high correlation (iii), the performance of the F-BSBL algorithm is practically the same as the performance of the oracle DOA-SBL algorithm which is given the true number of sources  $L$ . We refer the reader to [12] for a more in-depth investigation and discussion of the effects of the intra-block correlation  $D_i$  as well as for suggestions on how to estimate this matrix efficiently without introducing too many additional parameters.

Note, that in any practical example the DOAs will not align exactly with the search grid of potential DOAs. This mismatch introduces errors and complicates the estimation process. This can be counteracted e.g. by using a variational-EM approach similar to [35], [36] to optimizing the ELBO over the estimated source locations  $\hat{\theta}_l$  in addition to the variational parameters. Furthermore, [28] directly integrates the estimation of the parameters  $\hat{\theta}_l$  into the VB framework in order to obtain (approximate) posterior distributions  $q(\theta_l)$ . However, we consider these off-grid approaches outside the scope of this work.

## IX. CONCLUSION

We present a variational BSBL (VA-BSBL) algorithm and derive a fast version of it, called F-BSBL algorithm, that incorporates a fast update rule. To derive this fast update rule, we show that the procedure of sequentially updating the proxy PDF of the weights and the proxy PDF of a given hyperparameter can be expressed as a first-order recurrence relating the current and updated mean estimates of this hyperparameter. We show that the fixed points of the recurrent relation can be obtained as the roots of a polynomial for many commonly used hyperprior PDFs. Furthermore, by proving that the update-function of this recurrent relation is strictly increasing, we are able to determine if the sequence of mean estimates obtained by repeating *ad infinitum* the above update procedure converges and, if it does converge, we can determine its limit. Hence, we can check if the convergence criterion is met or if the sequence diverges and therefore update each hyperparameter mean estimate to its asymptotic value in a single step. Additionally, this convergence check allows to identify which parameter settings of the generalized inverse Gaussian hyperprior make this hyperprior sparsity promoting, i.e. they lead to an F-BSBL estimator incorporating a thresholding step, which is a mandatory condition for the estimator to be sparse.

Using numerical simulations, we show that the F-BSBL algorithm achieves a two orders of magnitude faster runtime compared to the BSBL-EM and BSBL-BO algorithms presented in [13]. Moreover, the F-BSBL algorithm is shown to achieve a smaller NMSE over a wide range of signal lengths, SNRs, block sizes and sparsity ratios than the benchmark algorithms. The F-BSBL algorithm is also applied to DOA estimation. Our results demonstrate that this algorithm (i) is able to outperform the SBL-based DOA estimation algorithm [19] in terms of computation time while achieving

a similar performance for single-snapshot DOA estimation and (ii) achieves a smaller OSPA than [19] in a low-SNR multiple-snapshot DOA estimation scenario where the source amplitudes are correlated over the snapshots.

We generalize the equivalence between variational SBL and EM-based Type-II SBL to the context of BSBL. Specifically, Theorem 3 shows that the EM-based Type-II-BSBL is equivalent to the VA-BSBL algorithm. Furthermore, this result also implies the equivalence between the fast versions of those algorithms, i.e. fast Type-II-BSBL using coordinate ascent for the former, e.g. [11], and the F-BSBL algorithm for the latter. This equivalence is conceptually relevant, since the VB approach presented herein can be given a message-passing interpretation in which messages are proxy PDFs.

Promising directions for future research are the extensions of the presented method and algorithms to include the estimation of the size of each block and to a parametrized continuous (infinite) dictionary matrix. For example, in the application of MMV-DOA estimation, the later extension would consist in dropping the restriction of the DOAs to a grid and estimate them instead by including an additional such stage in the proposed BSBL algorithms. Similar extensions of classical SBL are found e.g. in [29], [31], [35]–[37]. The aforementioned message-passing interpretation, which allows for combining the F-BSBL algorithm with other message-passing algorithms, like belief propagation [17], opens another interesting avenue for future research. Such combined message-passing algorithms could be used, e.g. for (i) joint channel estimation and decoding [18], [38], or (ii) sequential tracking of time-variant channels [39], especially in the context of multiple-input–multiple-output communication systems, as such channels are often modeled to be block-sparse [20], [21].

## APPENDIX

### A. Proof of Lemma 1

We aim to prove that the expectation  $\langle \mathbf{x}_i^H \mathbf{D}_i \mathbf{x}_i \rangle_{q_{\mathbf{x}}}$  in the update of  $\hat{\gamma}_i$  can be simplified into a rational function  $B_i(\hat{\gamma}_i)/A_i(\hat{\gamma}_i)$ . First, we find that

$$\langle \mathbf{x}_i^H \mathbf{D}_i \mathbf{x}_i \rangle_{q_{\mathbf{x}}} = \hat{\mathbf{x}}_i^H \mathbf{D}_i \hat{\mathbf{x}}_i + \text{tr}(\mathbf{D}_i \hat{\Sigma}_i) \quad (44)$$

is an expectation over a Gaussian PDF  $q_{\mathbf{x}}$ , where  $\hat{\Sigma}_i$  denotes the  $d_i \times d_i$  submatrix on the principal diagonal of  $\bar{\Sigma}$  corresponding to the (marginal) covariance of the  $i$ -th block  $\mathbf{x}_i$  in  $q_{\mathbf{x}}$  [40, Eq. (378)]. Let  $\mathbf{E}_i = [\mathbf{0} \ \mathbf{I}_{d_i} \ \mathbf{0}]^T$  be an  $M \times d_i$  selection matrix such that  $\hat{\mathbf{x}}_i = \mathbf{E}_i^T \hat{\mathbf{x}}$  and  $\hat{\Sigma}_i = \mathbf{E}_i^T \bar{\Sigma} \mathbf{E}_i$ , and let  $\mathbf{L}_i \mathbf{L}_i^H = \mathbf{D}_i$  be the Cholesky decomposition of  $\mathbf{D}_i$ .<sup>10</sup> Investigating the trace term

$$\text{tr}(\mathbf{D}_i \hat{\Sigma}_i) = \text{tr}(\mathbf{L}_i^H \mathbf{E}_i^T \bar{\Sigma} \mathbf{E}_i \mathbf{L}_i) \quad (45)$$

in (44), we make the dependence on  $\hat{\gamma}_i$  explicit by writing  $\hat{\Sigma}$  as

$$\hat{\Sigma} = (\bar{\Sigma}^{-1} + \hat{\gamma}_i \mathbf{E}_i \mathbf{D}_i \mathbf{E}_i^T)^{-1} \quad (46)$$

<sup>10</sup>For the case of  $\mathbf{D}_i = \text{diag}(\mathbf{b}_i)$  being a diagonal matrix with the elements of the vector  $\mathbf{b}_i$  on its main diagonal, the Cholesky decomposition results in the matrix  $\mathbf{L}_i = \text{diag}(\sqrt{\mathbf{b}_i})$ . Similarly, if  $\mathbf{D}_i = \mathbf{I}$  then it follows that  $\mathbf{L}_i = \mathbf{I}$ . Subsequently,  $\mathbf{L}_i$  can be removed from the definition of  $\mathbf{q}_i = \lambda \mathbf{U}_i^H \mathbf{E}_i^T \bar{\Sigma} \Phi^H \mathbf{y}$ , and  $\mathbf{s}_i$  are the eigenvalues of  $\bar{\Sigma}_i$ .

and applying the Woodbury matrix identity

$$\hat{\Sigma} = \bar{\Sigma} - \bar{\Sigma} \mathbf{E}_i (\hat{\gamma}_i^{-1} \mathbf{D}_i^{-1} + \bar{\Sigma}_i)^{-1} \mathbf{E}_i^T \bar{\Sigma} \quad (47)$$

where  $\bar{\Sigma} = (\lambda \Phi^H \Phi + \sum_{k=1, k \neq i}^K \hat{\gamma}_k \mathbf{E}_k \mathbf{D}_k \mathbf{E}_k^T)^{-1}$ , and  $\bar{\Sigma}_i = \mathbf{E}_i^T \bar{\Sigma} \mathbf{E}_i$ . Let  $\mathbf{U}_i \mathbf{S}_i \mathbf{U}_i^H$  be the eigendecomposition of  $\mathbf{L}_i^H \bar{\Sigma}_i \mathbf{L}_i$ , such that the columns of  $\mathbf{U}_i$  are the eigenvectors of  $\mathbf{L}_i^H \bar{\Sigma}_i \mathbf{L}_i$  and  $\mathbf{S}_i$  is a diagonal matrix with the corresponding eigenvalues  $s_{i,l}$  on its main diagonal and  $\mathbf{L}_i^H \bar{\Sigma}_i \mathbf{L}_i = \mathbf{U}_i \mathbf{S}_i \mathbf{U}_i^H$ . We insert (47) into (45) and use the identity

$$(\hat{\gamma}_i^{-1} \mathbf{D}_i^{-1} + \bar{\Sigma}_i)^{-1} = \mathbf{L}_i \mathbf{U}_i (\hat{\gamma}_i^{-1} \mathbf{I}_{d_i} + \mathbf{S}_i)^{-1} \mathbf{U}_i^H \mathbf{L}_i^H \quad (48)$$

to rewrite the trace term in (44) as

$$\begin{aligned} \text{tr}(\mathbf{D}_i \hat{\Sigma}_i) &= \text{tr}(\mathbf{S}_i) - \text{tr}(\mathbf{S}_i (\hat{\gamma}_i^{-1} \mathbf{I}_{d_i} + \mathbf{S}_i)^{-1} \mathbf{S}_i) \\ &= \sum_{l=1}^{d_i} \frac{s_{i,l}}{1 + \hat{\gamma}_i s_{i,l}}. \end{aligned} \quad (49)$$

Next, we investigate the expression  $\hat{\mathbf{x}}_i^H \mathbf{D}_i \hat{\mathbf{x}}_i$  in (44). Using (15), (47) and (48), we find

$$\begin{aligned} \hat{\mathbf{x}}_i^H \mathbf{D}_i \hat{\mathbf{x}}_i &= \hat{\lambda}^2 \mathbf{y}^H \Phi \bar{\Sigma} \mathbf{E}_i \mathbf{L}_i \mathbf{U}_i [\mathbf{I}_{d_i} - 2\mathbf{S}_i (\hat{\gamma}_i^{-1} \mathbf{I}_{d_i} + \mathbf{S}_i)^{-1} \\ &\quad + \mathbf{S}_i^2 (\hat{\gamma}_i^{-1} \mathbf{I}_{d_i} + \mathbf{S}_i)^{-2}] \mathbf{U}_i^H \mathbf{L}_i^H \mathbf{E}_i^T \bar{\Sigma} \Phi^H \mathbf{y} \end{aligned} \quad (50)$$

after applying a few algebraic manipulations. Equation (50) is a quadratic form  $\mathbf{q}_i^H \mathbf{A}_i \mathbf{q}_i$  of the vector

$$\mathbf{q}_i = \hat{\lambda} \mathbf{U}_i^H \mathbf{L}_i^H \mathbf{E}_i^T \bar{\Sigma} \Phi^H \mathbf{y} \quad (51)$$

and a diagonal matrix  $\mathbf{A}_i = \mathbf{I}_{d_i} - 2\mathbf{S}_i (\hat{\gamma}_i^{-1} \mathbf{I}_{d_i} + \mathbf{S}_i)^{-1} + \mathbf{S}_i^2 (\hat{\gamma}_i^{-1} \mathbf{I}_{d_i} + \mathbf{S}_i)^{-2}$ , which can be expressed as

$$\hat{\mathbf{x}}_i^H \mathbf{D}_i \hat{\mathbf{x}}_i = \sum_{l=1}^{d_i} \frac{|q_{i,l}|^2}{(1 + \hat{\gamma}_i s_{i,l})^2} \quad (52)$$

where  $q_{i,l}$  is the  $l$ -th entry of the vector  $\mathbf{q}_i$ .

We define the polynomial of degree  $2d_i$

$$A_i(\gamma) = \prod_{l=1}^{d_i} (1 + \gamma s_{i,l})^2 \quad (53)$$

and the polynomial of degree  $2d_i - 1$

$$B_i(\gamma) = \sum_{l=1}^{d_i} (\gamma s_{i,l}^2 + |q_{i,l}|^2 + s_{i,l}) \prod_{j=1, j \neq i}^{d_i} (1 + \gamma s_{i,j})^2. \quad (54)$$

Inserting (49) and (52) into (44), we arrive at  $\langle \mathbf{x}_i^H \mathbf{D}_i \mathbf{x}_i \rangle_{q_{\mathbf{x}}} = B_i(\hat{\gamma}_i)/A_i(\hat{\gamma}_i)$  after a few algebraic manipulations.

### B. Proof of Lemma 2

To obtain a more convenient expression for the rational function  $B_i(\gamma)/A_i(\gamma)$ , we express the polynomial  $B_i(\gamma)$  given in (54) as the product of  $A_i(\gamma)$  defined in (53) and some expression

$$B_i(\gamma) = \sum_{l=1}^{d_i} \frac{\gamma s_{i,l}^2 + |q_{i,l}|^2 + s_{i,l}}{(1 + \gamma s_{i,l})^2} \prod_{j=1}^{d_i} (1 + \gamma s_{i,j})^2. \quad (55)$$

Using (55), we find

$$\frac{B_i(\gamma)}{A_i(\gamma)} = \sum_{l=1}^{d_i} \frac{\gamma s_{i,l}^2 + |q_{i,l}|^2 + s_{i,l}}{(1 + \gamma s_{i,l})^2}. \quad (56)$$

Taking the derivative of (56) with respect to  $\gamma$  yields

$$\frac{d}{d\gamma} \frac{B_i(\gamma)}{A_i(\gamma)} = - \sum_{l=1}^{d_i} \frac{\gamma s_{i,l}^3 + 2s_{i,l}|q_{i,l}|^2 + s_{i,l}^2}{(1 + \gamma s_{i,l})^3}. \quad (57)$$

The variables  $s_{i,l}$  are the eigenvalues of a positive definite matrix and, thus,  $s_{i,l} > 0$ , resulting in  $\frac{d}{d\gamma} (B_i(\gamma)/A_i(\gamma)) < 0 \forall \gamma \in \mathbb{R}_{++}$ .

### C. Proof of Lemma 3

We aim to prove that

$$h_\alpha(u) = \frac{1}{\sqrt{u}} \frac{K_{\alpha+1}(\sqrt{u})}{K_\alpha(\sqrt{u})} \quad (58)$$

is strictly decreasing in  $u$ , i.e.

$$h'_\alpha(u) < 0. \quad (59)$$

Starting from [27, Eq. (9.6.26)]

$$K'_\alpha(z) = -K_{\alpha+1}(z) + \frac{\alpha}{z} K_\alpha(z) \quad (60)$$

a change of variables to  $z = \sqrt{u}$  and some algebraic manipulations yield

$$\frac{1}{\sqrt{u}} \frac{K_{\alpha+1}(\sqrt{u})}{K_\alpha(\sqrt{u})} = -2 \left[ \frac{K'_\alpha(\sqrt{u})}{K_\alpha(\sqrt{u})} - \frac{\alpha/2}{u} \right]. \quad (61)$$

Inserting  $\frac{K'_\alpha(\sqrt{u})}{K_\alpha(\sqrt{u})} = \frac{d}{du} \ln K_\alpha(\sqrt{u})$  and  $-\frac{\alpha/2}{u} = \frac{d}{du} \ln u^{-\alpha/2}$ , we find

$$h_\alpha(u) = \frac{d}{du} \left[ -2 \ln (u^{-\alpha/2} K_\alpha(\sqrt{u})) \right] \triangleq k'(u) \quad (62)$$

where we defined  $k(u) = -2 \ln (u^{-\alpha/2} K_\alpha(\sqrt{u}))$ .

From (62) follows, that the condition (59) is equivalent to

$$k''(u) < 0 \quad (63)$$

i.e. that  $h_\alpha(u)$  is strictly decreasing if, and only if,  $k(u)$  is strictly concave. We write  $k(u) = k_1 \circ k_2(u)$  as the composition of  $k_1(v) = -2 \ln v$  and  $k_2(u) = u^{-\alpha/2} K_\alpha(\sqrt{u})$  to find

$$k''(u) = k''_1(k_2(u)) \cdot k'_2(u)^2 + k'_1(k_2(u)) \cdot k''_2(u) \quad (64)$$

Inserting  $k'_1(v) = -\frac{2}{v}$  and  $k''_1(v) = \frac{2}{v^2}$  we find

$$k''(u) = 2 \frac{k'_2(u)}{k_2(u)} \left[ \frac{k'_2(u)}{k_2(u)} - \frac{k''_2(u)}{k'_2(u)} \right]. \quad (65)$$

Using [27, Eq. (9.6.28)], we find the derivatives  $k'_2(u)$  and  $k''_2(u)$  as

$$k'_2(u) = -\frac{1}{2} u^{-(\alpha+1)/2} K_{\alpha+1}(\sqrt{u}) \quad (66)$$

$$k''_2(u) = \frac{1}{4} u^{-(\alpha+2)/2} K_{\alpha+2}(\sqrt{u}) \quad (67)$$

resulting in the expressions

$$\frac{k'_2(u)}{k_2(u)} = -\frac{1}{2} u^{-1/2} R_\alpha(\sqrt{u}) \quad (68)$$

$$\frac{k''_2(u)}{k'_2(u)} = -\frac{1}{2} u^{-1/2} R_{\alpha+1}(\sqrt{u}) \quad (69)$$

where  $R_\alpha(z) = \frac{K_{\alpha+1}(z)}{K_\alpha(z)}$ . For  $z > 0$ , the function  $R_\alpha(z)$  is positive and increasing with respect to  $\alpha$  [41, Lemma 2.2]. Thus, inserting (68) and (69) into (65), we arrive at

$$k''(u) = -\frac{1}{2} u^{-1} R_\alpha(\sqrt{u}) [R_{\alpha+1}(\sqrt{u}) - R_\alpha(\sqrt{u})] < 0. \quad (70)$$

### D. Conditions for the Convex Representation

We aim to show that the prior  $p(\mathbf{x}_i)$  in (8) admits the convex representation (32). Defining  $\alpha = -(c + \rho d_i)$ , we write (8) as

$$p(\mathbf{x}_i) \propto \left( \sqrt{b(a+z^2)} \right)^\alpha K_\alpha \left( \sqrt{b(a+z^2)} \right) \quad (71)$$

with  $z = \sqrt{\mathbf{x}_i^H \mathbf{D}_i \mathbf{x}_i}$ . Hence,  $p(\mathbf{x}_i)$  in (8) can be written as  $p(\mathbf{x}_i) = \exp(-g(z^2))$ , where

$$g(z) = -\frac{\alpha}{2} \ln(b(a+z)) - \ln K_\alpha(\sqrt{b(a+z)}) + \text{const}. \quad (72)$$

We show now that  $g(z)$  is increasing and concave. Calculating the derivative of  $g(z)$ , we find

$$g'(z) = \frac{b}{2} \left( \sqrt{b(a+z)} R_{\alpha-1}(\sqrt{b(a+z)}) \right)^{-1} \quad (73)$$

using [27, Eq. (9.6.26)] and  $K_\alpha(u)/K_{\alpha-1}(u) \triangleq R_{\alpha-1}(u)$ . Thus,  $g(z)$  is increasing since  $R_\alpha$  is positive on  $(0, \infty)$  [22].

Writing (73) as the composition

$$g'(z) = \frac{b}{2} k_\alpha^{-1} \circ u(z) \quad (74)$$

of the two functions  $u(z) = \sqrt{b(a+z)}$  and  $k_\alpha(u) = u R_{\alpha-1}(u)$ , we obtain the second derivative as

$$g''(z) = -\frac{b}{2} k_\alpha(u(z))^{-2} \cdot k'_\alpha(u(z)) \cdot u'(z) \quad (75)$$

where  $k'_\alpha$  and  $u'$  are the first derivatives of  $k_\alpha$  and  $u$ , respectively. The function  $k_\alpha$  is increasing for any real  $\alpha$ , i.e.  $k'_\alpha(u) > 0$  [41, Lemma 2.6]. Thus,  $g(z)$  is concave since  $k_\alpha(u) > 0$  and  $u'(z) > 0$  also hold for any  $u, z \in (0, \infty)$ .

### E. Detailed Derivations for Theorem 3

First, we investigate the EM algorithm based on the convex representation (32) of the prior  $p(\mathbf{x}_i)$ . Inserting  $p(\mathbf{x}_i; \gamma_i) = \mathcal{N}(\mathbf{x}_i; \mathbf{0}, (\gamma \mathbf{D}_i)^{-1})$  into (32), we find

$$-\ln p(\mathbf{x}_i) = -\rho \ln \left| \frac{\rho}{\pi} \mathbf{D}_i \right| + h_i(u_i) \quad (76)$$

after some algebraic manipulations, where  $u_i = u_i(\mathbf{x}_i) = \rho \mathbf{x}_i^H \mathbf{D}_i \mathbf{x}_i$ , and

$$h_i(u_i) \triangleq \inf_{\gamma_i} \left\{ u_i \gamma_i - \underbrace{\rho d_i \ln \gamma_i - \ln \varphi(\gamma_i)}_{\triangleq -h_i^*(\gamma_i)} \right\} \quad (77)$$

is a concave function of  $u_i$  with dual  $h_i^*(\gamma_i)$ .

Let  $\tilde{\gamma}_i = [\hat{\gamma}_1 \hat{\gamma}_2 \cdots \hat{\gamma}_{i-1} \gamma_i \hat{\gamma}_{i+1} \cdots \hat{\gamma}_K]^T$ , we insert  $q_{\text{EM}}(\mathbf{x}) = \mathcal{N}(\mathbf{x}; \hat{\mathbf{x}}, \hat{\Sigma})$ , with  $\hat{\mathbf{x}}$  and  $\hat{\Sigma}$  given by (15) into (36), to find

$$\begin{aligned} \hat{\gamma}_{i,\text{EM}} &= \arg \max_{\gamma_i} Q(\tilde{\gamma}_i, q_{\text{EM}}(\mathbf{x})) \\ &= \arg \min_{\gamma_i} \left\{ \gamma_i \rho \langle \mathbf{x}_i^H \mathbf{D}_i \mathbf{x}_i \rangle_{q_{\text{EM}}(\mathbf{x})} \right. \\ &\quad \left. - \rho d_i \ln \gamma_i - \ln \varphi(\gamma_i) \right\} \\ &= \arg \min_{\gamma_i} \{ u_i \gamma_i - h_i^*(\gamma_i) \}. \end{aligned} \quad (78)$$

where  $u_i = \rho \langle \mathbf{x}_i^H \mathbf{D}_i \mathbf{x}_i \rangle_{q_{\text{EM}}(\mathbf{x})}$ . To find the minimum of (78), we set the first derivative to zero  $\frac{d}{d\gamma_i}(u_i \gamma_i - h_i^*(\gamma_i)) = 0$ , resulting in

$$\hat{\gamma}_{i,\text{EM}} = h_i'(u_i). \quad (79)$$

Next, we turn to the VB algorithm. From the VB update rule (12), we find

$$q_{\gamma_i}(\gamma_i) \propto \exp \langle \ln p(\gamma_i | \mathbf{x}_i) \rangle_{q_{\mathbf{x}}(\mathbf{x})} \quad (80)$$

After a few algebraic manipulations, where

$$p(\gamma_i | \mathbf{x}_i) \propto \gamma_i^{\rho d_i} \exp\{-\rho \mathbf{x}_i^H \mathbf{D}_i \mathbf{x}_i\} \cdot p(\gamma_i). \quad (81)$$

Note, that  $p(\gamma_i | \mathbf{x}_i)$  depends on  $\mathbf{x}_i$  only via the value  $u_i(\mathbf{x}_i) = \rho \mathbf{x}_i^H \mathbf{D}_i \mathbf{x}_i$ . Similarly, from (80) we find that  $q_{\gamma_i}$  is parameterized by  $q_{\mathbf{x}}$  only through the expectation  $u_i(q_{\mathbf{x}}) = \rho \langle \mathbf{x}_i^H \mathbf{D}_i \mathbf{x}_i \rangle_{q_{\mathbf{x}}(\mathbf{x})}$ . Hence, the distributions  $p(\gamma_i | \mathbf{x}_i)$  and  $q_{\gamma_i}(\gamma_i)$  can both be written as a parameterized distribution

$$p(\gamma_i; u_i) \propto \gamma_i^{\rho d_i} \exp\{-u_i \gamma_i\} p(\gamma_i) \quad (82)$$

parameterized either by  $u_i = u_i(\mathbf{x}_i) = \rho \mathbf{x}_i^H \mathbf{D}_i \mathbf{x}_i$  or  $u_i = u_i(q_{\mathbf{x}}) = \rho \langle \mathbf{x}_i^H \mathbf{D}_i \mathbf{x}_i \rangle_{q_{\mathbf{x}}}$ , respectively. Therefore, the VB update  $\hat{\gamma}_i = \langle \gamma_i \rangle_{q_{\gamma_i}}$  is equivalent to the EM update (79) if, and only if,  $\langle \gamma_i \rangle_{p(\gamma_i; u_i)} = h_i'(u_i)$ .

To show that indeed  $\langle \gamma_i \rangle_{p(\gamma_i; u_i)} = h_i'(u_i)$ , we first introduce some intermediary results. Using the rules of differentiating under the integral and standard vector calculus, it can be shown that

$$\nabla p(\mathbf{x}_i | \gamma_i) = -\gamma_i \mathbf{D}_i \mathbf{x}_i p(\mathbf{x}_i | \gamma_i) \quad (83)$$

where  $\nabla$  denotes the Nabla-operator (with respect to the vector  $\mathbf{x}_i$ ). Using  $p(\mathbf{x}_i) = \int p(\mathbf{x}_i | \gamma_i) p(\gamma_i) d\gamma_i$ , we find

$$\nabla p(\mathbf{x}_i) = -\mathbf{D}_i \mathbf{x}_i p(\mathbf{x}_i) \cdot \langle \gamma_i \rangle_{p(\gamma_i | \mathbf{x}_i)}. \quad (84)$$

Rewriting (76) as composition

$$p(\mathbf{x}_i) = \left(\frac{\rho}{\pi}\right)^{\rho d_i} |\mathbf{D}_i|^\rho \exp\{-h_i(u_i)\} \circ u_i(\mathbf{x}_i) \quad (85)$$

where  $u_i(\mathbf{x}_i) = \rho \mathbf{x}_i^H \mathbf{D}_i \mathbf{x}_i$ , we calculate the gradient to find

$$\nabla p(\mathbf{x}_i) = -\mathbf{D}_i \mathbf{x}_i p(\mathbf{x}_i) \cdot h_i'(u_i)|_{u_i = \rho \mathbf{x}_i^H \mathbf{D}_i \mathbf{x}_i}. \quad (86)$$

Combining (84) with (86), we find

$$\langle \gamma_i \rangle_{p(\gamma_i | \mathbf{x}_i)} = h_i'(u_i(\mathbf{x}_i)) \quad (87)$$

Thus,

$$\hat{\gamma}_i = \langle \gamma_i \rangle_{q_{\gamma_i}} = h_i'(u_i) \quad (88)$$

where  $u_i = u_i(q_{\mathbf{x}}) = \rho \langle \mathbf{x}_i^H \mathbf{D}_i \mathbf{x}_i \rangle_{q_{\mathbf{x}}}$ .

## F. Equivalence Between F-BSBL and Fast Type-II-BSBL

The first step in proving the equivalence between the fast Type-II-BSBL [11] and F-BSBL is expressing the Type-II marginal likelihood (35) as

$$2 \ln \tilde{p}(\mathbf{y}; \boldsymbol{\gamma}) = \ln |\boldsymbol{\Sigma}| + \hat{\boldsymbol{\lambda}}^2 \mathbf{y}^H \boldsymbol{\Phi} \boldsymbol{\Sigma} \boldsymbol{\Phi}^H \mathbf{y} + \sum_{i=1}^K d_i \ln \gamma_i + \text{const.} \quad (89)$$

after integrating out the weights  $\mathbf{x}$ .

Let  $\boldsymbol{\Phi}_i$  denote all columns of the dictionary matrix which correspond to the  $i$ -th block and  $\boldsymbol{\Phi}_{\sim i}$  all remaining columns of  $\boldsymbol{\Phi}$ , such that  $\boldsymbol{\Phi} = [\boldsymbol{\Phi}_{\sim i} \boldsymbol{\Phi}_i]$ . Similarly, let  $\mathbf{D}_{\sim i}$  be a diagonal matrix with the blocks  $\gamma_k \mathbf{D}_k \forall k \in \{1, 2, \dots, K\} \setminus \{i\}$  on its main diagonal, such that we can express  $\boldsymbol{\Sigma}^{-1}$  as a block matrix<sup>11</sup>

$$\boldsymbol{\Sigma}^{-1} = \begin{bmatrix} \lambda \boldsymbol{\Phi}_{\sim i}^H \boldsymbol{\Phi}_{\sim i} + \mathbf{D}_{\sim i} & \lambda \boldsymbol{\Phi}_{\sim i}^H \boldsymbol{\Phi}_i \\ \lambda \boldsymbol{\Phi}_i^H \boldsymbol{\Phi}_{\sim i} & \lambda \boldsymbol{\Phi}_i^H \boldsymbol{\Phi}_i + \gamma_i \mathbf{I} \end{bmatrix}. \quad (90)$$

Denoting  $\boldsymbol{\Sigma}_{\sim i} = (\lambda \boldsymbol{\Phi}_{\sim i}^H \boldsymbol{\Phi}_{\sim i} + \mathbf{D}_{\sim i})^{-1}$  and  $\boldsymbol{\Sigma}_i = (\lambda \boldsymbol{\Phi}_i^H \boldsymbol{\Phi}_i - \lambda^2 \boldsymbol{\Phi}_i^H \boldsymbol{\Phi}_{\sim i} \boldsymbol{\Sigma}_{\sim i} \boldsymbol{\Phi}_{\sim i}^H \boldsymbol{\Phi}_i)^{-1}$ , we use the block matrix determinant lemma to express

$$\begin{aligned} \ln |\boldsymbol{\Sigma}| &= -\ln |\boldsymbol{\Sigma}^{-1}| = \ln |\boldsymbol{\Sigma}_{\sim i}| - \ln |\boldsymbol{\Sigma}_i^{-1} + \gamma_i \mathbf{I}| \\ &= \ln |\boldsymbol{\Sigma}_{\sim i}| - \sum_{l=1}^{d_i} \ln \left( \gamma_i + \frac{1}{s_{i,l}} \right). \end{aligned} \quad (91)$$

Using the Woodbury matrix identity, we can also make the dependence on  $\gamma_i$  explicit in the second term in (89)

$$\lambda^2 \mathbf{y}^H \boldsymbol{\Phi} \boldsymbol{\Sigma} \boldsymbol{\Phi}^H \mathbf{y} = \lambda^2 \mathbf{y}^H \boldsymbol{\Phi} (\bar{\boldsymbol{\Sigma}} - \bar{\boldsymbol{\Sigma}} \mathbf{E}_i (\gamma_i^{-1} \mathbf{I} + \boldsymbol{\Sigma}_i)^{-1} \mathbf{E}_i^T \bar{\boldsymbol{\Sigma}}) \boldsymbol{\Phi}^H \mathbf{y} \quad (92)$$

Using the identity (48), expression (92) can be further simplified to

$$\begin{aligned} \lambda^2 \mathbf{y}^H \boldsymbol{\Phi} \boldsymbol{\Sigma} \boldsymbol{\Phi}^H \mathbf{y} &= \text{const.} - \mathbf{q}_i^H (\gamma_i^{-1} \mathbf{I} + \mathbf{S}_i)^{-1} \mathbf{q}_i \\ &= \text{const.} - \sum_{l=1}^{d_i} \frac{\gamma_i |q_{i,l}|^2}{1 + \gamma_i s_{i,l}}. \end{aligned} \quad (93)$$

Inserting (91) and (93) into (89) we arrive at

$$2 \ln \tilde{p}(\mathbf{y}; \boldsymbol{\gamma}) = \mathcal{L}_{\sim i}(\boldsymbol{\gamma}_{\sim i}) + \sum_{l=1}^{d_i} \ln \left( \frac{\gamma_i s_{i,l}}{1 + \gamma_i s_{i,l}} \right) - \frac{\gamma_i |q_{i,l}|^2}{(1 + \gamma_i s_{i,l})^2} \quad (94)$$

where  $s_{i,l}$  and  $q_{i,l}$  are the quantities defined in Appendix A,  $\boldsymbol{\gamma}_{\sim i}$  denotes the vector  $\boldsymbol{\gamma}$  with the element  $\gamma_i$  removed, and  $\mathcal{L}_{\sim i}(\boldsymbol{\gamma}_{\sim i})$  is some function which does not depend on  $\gamma_i$ .

The maximum of the marginal likelihood (94) must fulfill  $\mathcal{L}'_i(\gamma_i) = 0$ . The derivative of (94) is

$$\mathcal{L}'_i(\gamma_i) = \sum_{l=1}^{d_i} \frac{1}{\gamma_i} \frac{1}{1 + \gamma_i s_{i,l}} - \frac{|q_{i,l}|^2}{(1 + \gamma_i s_{i,l})^2} \quad (95)$$

Inserting (95) into the condition  $\mathcal{L}'_i(\gamma_i) = 0$  and multiply both sides of the equation with  $\gamma_i \prod_{l=1}^{d_i} (1 + \gamma_i s_{i,l})^2$  yields

$$0 = \gamma_i B_i(\gamma_i) - d_i A_i(\gamma_i) \quad (96)$$

<sup>11</sup>We use  $\mathbf{D}_i = \mathbf{I}$  to simplify the notation, but the results can be easily verified to applied to the case of a general  $\mathbf{D}_i$  as well.

after a some algebraic manipulations, where  $A_i(\gamma_i)$  and  $B_i(\gamma)$  are the polynomials defined in (53) and (54), respectively. Comparing (96) with the polynomials  $G_i(\gamma)$  in the last row and fifth column of Table I, we recognize that the extrema of the marginalized likelihood with respect to a single  $\gamma_i$  correspond to the fixed points of the recurrent relation in the fast VB solution in case Jeffrey's prior is used.

## REFERENCES

- [1] M. F. Duarte and Y. C. Eldar, "Structured compressed sensing: From theory to applications," *IEEE Trans. Signal Process.*, vol. 59, no. 9, pp. 4053–4085, Sep. 2011.
- [2] O. Barndorff-Nielsen, J. Kent, and M. Sørensen, "Normal variance-mean mixtures and z distributions," *Int. Statist. Rev. / Revue Internationale de Statistique*, vol. 50, no. 2, pp. 145–159, Aug. 1982.
- [3] M. E. Tipping, "Sparse Bayesian learning and the relevance vector machine," *J. Mach. Learn. Res.*, vol. 1, pp. 211–244, Jun. 2001.
- [4] D. P. Wipf and B. D. Rao, "Sparse Bayesian learning for basis selection," *IEEE Trans. Signal Process.*, vol. 52, no. 8, pp. 2153–2164, Aug. 2004.
- [5] D. Shutin, T. Buchgraber, S. R. Kulkarni, and H. V. Poor, "Fast variational sparse Bayesian learning with automatic relevance determination for superimposed signals," *IEEE Trans. Signal Process.*, vol. 59, no. 12, pp. 6257–6261, Dec. 2011.
- [6] D. P. Wipf, B. D. Rao, and S. Nagarajan, "Latent variable Bayesian models for promoting sparsity," *IEEE Trans. Inf. Theory*, vol. 57, no. 9, pp. 6236–6255, Sep. 2011.
- [7] A. Faul and M. Tipping, "Analysis of sparse Bayesian learning," in *Advances Neural Inf. Process. Syst.*, vol. 14, Vancouver, Canada, Dec. 3–8, 2001, pp. 383–389.
- [8] M. E. Tipping and A. C. Faul, "Fast marginal likelihood maximisation for sparse Bayesian models," in *Proc. 9th Int. Workshop Artif. Intell. and Statist.*, vol. R4, Key West, FL, USA, Jan. 03–06, 2003, pp. 276–283.
- [9] N. L. Pedersen, C. Navarro Manchón, M.-A. Badiu, D. Shutin, and B. H. Fleury, "Sparse estimation using Bayesian hierarchical prior modeling for real and complex linear models," *Signal Process.*, vol. 115, pp. 94–109, Oct. 2015.
- [10] M. Luessi, S. D. Babacan, R. Molina, and A. K. Katsaggelos, "Bayesian simultaneous sparse approximation with smooth signals," *IEEE Trans. Signal Process.*, vol. 61, no. 22, pp. 5716–5729, Nov. 2013.
- [11] Z. Ma, W. Dai, Y. Liu, and X. Wang, "Group sparse Bayesian learning via exact and fast marginal likelihood maximization," *IEEE Trans. Signal Process.*, vol. 65, no. 10, pp. 2741–2753, May 2017.
- [12] Z. Zhang and B. D. Rao, "Sparse signal recovery with temporally correlated source vectors using sparse Bayesian learning," *IEEE J. Sel. Topics Signal Process.*, vol. 5, no. 5, pp. 912–926, 2011.
- [13] —, "Extension of SBL algorithms for the recovery of block sparse signals with intra-block correlation," *IEEE Trans. Signal Process.*, vol. 61, no. 8, pp. 2009–2015, Apr. 2013.
- [14] S. D. Babacan, S. Nakajima, and M. N. Do, "Bayesian group-sparse modeling and variational inference," *IEEE Trans. Signal Process.*, vol. 62, no. 11, pp. 2906–2921, Jun. 2014.
- [15] S. Sharma, S. Chaudhury, and Jayadeva, "Variational Bayes block sparse modeling with correlated entries," in *24th Int. Conf. Pattern Recognit.*, Beijing, China, Aug. 20–24, 2018, pp. 1313–1318.
- [16] J. Palmer, K. Kreutz-Delgado, B. Rao, and D. Wipf, "Variational EM algorithms for non-Gaussian latent variable models," in *Adv. Neural Inf. Process. Syst.*, vol. 18, Vancouver, Canada, Dec. 5–8, 2005, pp. 1059–1066.
- [17] E. Riegler, G. E. Kirkelund, C. N. Manchon, M. A. Badiu, and B. H. Fleury, "Merging belief propagation and the mean field approximation: A free energy approach," *IEEE Trans. Inf. Theory*, vol. 59, no. 1, pp. 588–602, Jan. 2013.
- [18] T. L. Hansen, P. B. Jørgensen, M.-A. Badiu, and B. H. Fleury, "An iterative receiver for OFDM with sparsity-based parametric channel estimation," *IEEE Trans. Signal Process.*, vol. 66, no. 20, pp. 5454–5469, Oct. 2018.
- [19] P. Gerstoft, C. F. Mecklenbräuker, A. Xenaki, and S. Nannuru, "Multisnapshot sparse Bayesian learning for DOA," *IEEE Signal Process. Lett.*, vol. 23, no. 10, pp. 1469–1473, Oct. 2016.
- [20] O.-E. Barbu, C. Navarro Manchón, C. Rom, T. Balercia, and B. H. Fleury, "OFDM receiver for fast time-varying channels using block-sparse Bayesian learning," *IEEE Trans. Veh. Technol.*, vol. 65, no. 12, pp. 10 053–10 057, Dec. 2016.
- [21] R. Prasad, C. R. Murthy, and B. D. Rao, "Joint channel estimation and data detection in MIMO-OFDM systems: A sparse Bayesian learning approach," *IEEE Trans. Signal Process.*, vol. 63, no. 20, pp. 5369–5382, Oct. 2015.
- [22] B. Jørgensen, *Statistical properties of the generalized inverse Gaussian distribution*, ser. Lecture notes in statistics. New York, NY, USA: Springer-Verlag, 1982, vol. 9.
- [23] D. G. Tzikas, A. C. Likas, and N. P. Galatsanos, "The variational approximation for Bayesian inference," *IEEE Signal Process. Mag.*, vol. 25, no. 6, pp. 131–146, Nov. 2008.
- [24] C. M. Bishop, *Pattern Recognition and Machine Learning*. Secaucus, NJ, USA: Springer-Verlag New York, Inc., 2006.
- [25] W. Rudin, *Principles of mathematical analysis*, 3rd ed. New York, NY, USA: McGraw-Hill, 1976.
- [26] A. Edelman and H. Murakami, "Polynomial roots from companion matrix eigenvalues," *Math. Comput.*, vol. 64, no. 210, pp. 763–776, 1995.
- [27] M. Abramowitz and I. A. Stegun, *Handbook of Mathematical Functions*, 10th ed. National Bureau of Standards, 1972.
- [28] M.-A. Badiu, T. L. Hansen, and B. H. Fleury, "Variational Bayesian inference of line spectra," *IEEE Trans. Signal Process.*, vol. 65, no. 9, pp. 2247–2261, May 2017.
- [29] T. L. Hansen, B. H. Fleury, and B. D. Rao, "Superfast line spectral estimation," *IEEE Trans. Signal Process.*, vol. 66, no. 10, pp. 2511–2526, Feb. 2018.
- [30] E. Leitinger, S. Grebien, B. Fleury, and K. Witrisal, "Detection and estimation of a spectral line in MIMO systems," in *2020 54th Asilomar Conf. Signals, Syst. and Computers*, Pacific Grove, CA, USA, Nov. 01–04, 2020, pp. 1090–1095.
- [31] S. Grebien, E. Leitinger, K. Witrisal, and B. H. Fleury, "Super-resolution estimation of UWB channels including the dense component – An SBL-inspired approach," *IEEE Trans. Wireless Commun.*, vol. 23, no. 8, pp. 10 301–10 318, Feb. 2024.
- [32] D. Wipf, J. Palmer, B. Rao, and K. Kreutz-Delgado, "Performance evaluation of latent variable models with sparse priors," in *2007 IEEE Int. Conf. Acoust., Speech and Signal Process.*, Honolulu, HI, USA, Apr. 15–20, 2007.
- [33] D. Schuhmacher, B.-T. Vo, and B.-N. Vo, "A consistent metric for performance evaluation of multi-object filters," *IEEE Trans. Signal Process.*, vol. 56, no. 8, pp. 3447–3457, Aug. 2008.
- [34] Y. Park, F. Meyer, and P. Gerstoft, "Graph-based sequential beamforming," *J. Acoustical Soc. Amer.*, vol. 153, no. 1, pp. 723–737, Jan. 2023.
- [35] D. Shutin, W. Wand, and T. Jost, "Incremental sparse Bayesian learning for parameter estimation of superimposed signals," in *10th Int. Conf. Sampling Theory and Appl.*, Bremen, Germany, Jul. 1–5, 2013, pp. 513–516.
- [36] J. Möderl, F. Pernkopf, K. Witrisal, and E. Leitinger, "Variational inference of structured line spectra exploiting group-sparsity," *ArXiv e-prints*, Mar. 2023. [Online]. Available: <https://arxiv.org/abs/2303.03017>
- [37] T. L. Hansen, M. A. Badiu, B. H. Fleury, and B. D. Rao, "A sparse Bayesian learning algorithm with dictionary parameter estimation," in *2014 IEEE 8th Sensor Array and Multichannel Signal Process. Workshop (SAM)*, A Coruna, Spain, Jun. 22–25, 2014, pp. 385–388.
- [38] G. E. Kirkelund, C. N. Manchon, L. P. B. Christensen, E. Riegler, and B. H. Fleury, "Variational message-passing for joint channel estimation and decoding in MIMO-OFDM," in *2010 IEEE Global Telecommun. Conf.*, London, U.K., Dec. 6–10, 2010, pp. 1–6.
- [39] X. Li, E. Leitinger, A. Venus, and F. Tufvesson, "Sequential detection and estimation of multipath channel parameters using belief propagation," *IEEE Trans. Wireless Commun.*, vol. 21, no. 10, pp. 8385–8402, Oct. 2022.
- [40] K. B. Petersen and M. S. Pedersen, *The Matrix Cookbook*. Technical University of Denmark, 2012, version Nov. 15, 2012, Accessed: Oct. 2023. [Online]. Available: <https://www.math.uwaterloo.ca/~hwolkowi/matrixcookbook.pdf>
- [41] M. E. H. Ismail and M. E. Muldoon, "Monotonicity of the zeros of a cross-product of Bessel functions," *SIAM J. Math. Anal.*, vol. 9, no. 4, pp. 759–767, 1978.